Computer Resolution of Overlapping Electronic Absorption Bands

By Barry E. Barker
COMPUTER CENTRE, LEICESTER POLYTECHNIC, LEICESTER LE1 9BH
and Malcolm F. Fox
SCHOOL OF CHEMISTRY, LEICESTER POLYTECHNIC, LEICESTER LE1 9BH

1 Introduction

It is a simple procedure to obtain electronic spectra from spectrophotometers. Figure 1a shows the absorption spectrum of very dilute hydrosulphide ion in acetone at 208 K.[1] This spectrum is typical in being broad and unstructured with several bands obvious to initial inspection. The problem lies in that whilst each absorption band contains information of both inter- and intra-molecular transitions, overall giving a detailed system description, the poor resolution of the bands prevents a simple, straightforward, and unique solution for the band parameters. The poor resolution arises from overlap of broad absorption bands, the breadth of the bands arising from a wide distribution of internal and external perturbations. To investigate a spectrum such as that in Figure 1a, workers have increasingly turned to 'computer analysis' of various forms to determine accurately the position, height, and width for each band contributing to complex absorption profiles. These analyses are the subject of this review—the computer analysis of electronic absorption spectra which are linear combinations of overlapping band shapes.

The resolution of electronic band profiles has been overshadowed by the considerable emphasis given to computer analysis of i.r. and Raman spectra, as exemplified by the work of Jones *et al.*[2] These areas have quite different properties when considered for computer analysis. For u.v.–visible spectra, the band shape is different, halfwidths are much wider (by up to two orders of magnitude) the bands are more overlapped but very much fewer in number than for vibrational spectra. Instrumental conditions are also different in that u.v.–visible spectra are usually obtained at high signal-to-noise ratios, with good instrumental resolution and accurate knowledge of the base-line. Noise from all sources is therefore reduced (but not removed), instrumental slit function distortion of the spectrum is minimized and accurate intensities can be assumed.

Computer resolution of band profiles has many facets. One problem may be fitting a complex shape function, such as the Voigt function, to one band to

[1] M. F. Fox and E. Hayon, *J. Chem. Soc., Faraday Trans.* 1, 1979, **75**, 1380.
[2] R. N. Jones, *Pure Appl. Chem.*, 1969, **18**, 303.

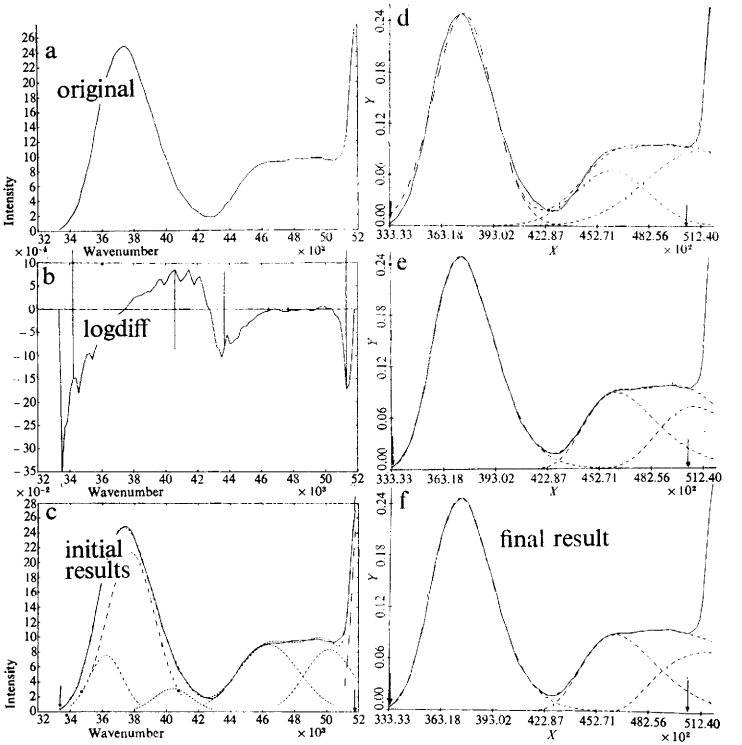

Figure 1 *All full line spectra show the actual spectrum. Broken lines represent the individual bands and also their summation.* (a) *The initial spectrum of tetra-n-butylammonium hydrosulphide in acetone at* 208 K, *concentration* 2.5 × 10^{-3} mol dm^{-3}, *from ref.* 1. (b) *The LOGDIFF transform of* (a) *above, ref.* 6. (c) *The six bands resolved from* (a) *above using the LOGDIFF interactive method.* (d) *The optimized three Gaussian band solution.* (e) *The initial optimized three log-normal band solution.* (f) *The finally optimized three log-normal band solution, iterated to optimal values after the values of* (e) *above have been linearized with reference to spectra similarly analysed at* 230, 253, 273, 289, *and* 318 K

extremely high accuracy using very large and powerful computing facilities.[3] On the other hand, a relatively small computer may be used to resolve a linear combination of up to six separate bands with simple shape functions contributing to a complex absorption profile.[4] In this way, an investigator's perception of the overall problem is often framed through the nature of his or her own problem, the instruments available, and the computing facilities available. There is a variety of methods, *e.g.* in Figure 1a we may visually estimate the Gaussian band parameters, measure the band parameters by graphical construction, or use an

[3] T. Sundius, *J. Raman Spectrosc.*, 1973, **1**, 471.
[4] B. E. Barker, M. F. Fox, E. Hayon, and A. Walton, *J. Chem. Soc., Faraday Trans.* 1, 1976, **72**, 1990.

analogue synthesizer.[5] Alternatively, a method of numerical analysis such as the LOGDIFF method[6] may be used repetitively to give a solution based on six possible bands, Figure 1c. Various considerations lead us to a four band Gaussian solution, a three band Gaussian solution, Figure 1d, and a three log-normal band solution, Figure 1e. Reference to other spectra of hydrosulphide in acetone at other temperatures leads to a final solution, Figure 1f. Figures 1d—1f have solutions achieved using computer convergence methods. The techniques and philosophy used to analyse the spectrum are described below.

What can be done with the information which has been obtained? Accurate knowledge of the individual band parameters in an absorption/emission profile gives information about ground and excited states, *e.g.* from previously unrecognised vibronic coupling as in the example shown in Figure 2. The effects of

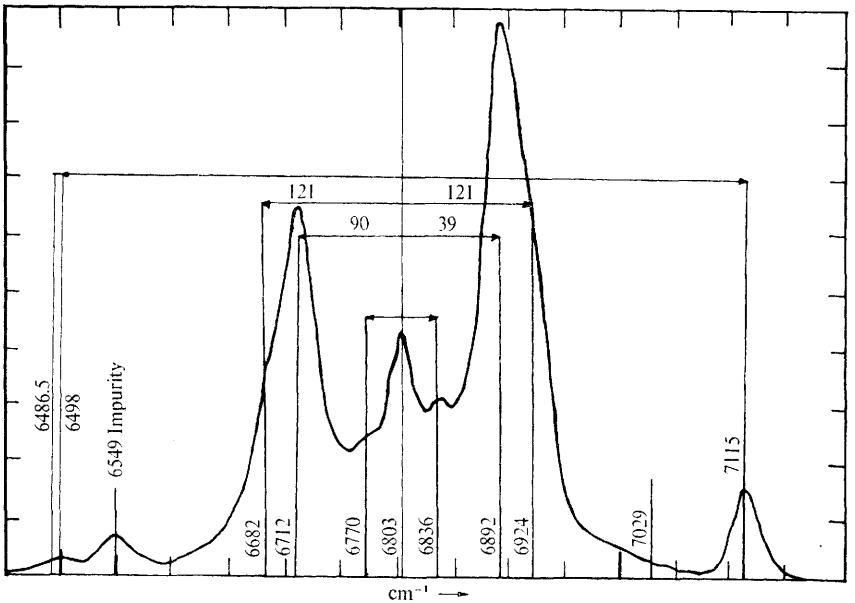

Figure 2 *Electronic spectrum of tetraphenylarsonium uranium hexachloride, with some* U^{IV} *impurity at* 6549 cm^{-1}. *The band at* 6803 cm^{-1} *is a forbidden electronic transition and the other structure is vibronic, hence its periodic nature*
(Reproduced by permission from *Anal. Chem.*, 1968, **40**, 905)

pH, temperature, and pressure on complex equilibria may be accurately determined.[7] The accurate, but succinct, reporting of electronic absorption spectra may be reduced to a small number of parameters rather than reproducing

[5] Du Pont Nemours Company, Delaware, U.S.A.
[6] B. E. Barker, M. F. Fox, E. Hayon, and E. M. Ross, *Analyt. Chem.*, 1974, **46**, 1785.
[7] T. R. Griffiths *et al.*, *J. Inorg. Nucl. Chem.*, 1975, **37**, 511, 521; *J. Chem. Soc., Dalton Trans* 1975, 344.

a spectrum—expensive of both journal space and production cost. Jones has demonstrated data compression, at the same time preserving a very good representation of an i.r. spectrum, from 7040 ordinates to 193 spectral indices for cyclohexane.[2]

These approaches match trends in the development of spectrophotometers, for already microprocessors are being used for instrumental control functions and elementary data processing. We expect further developments in realtime data processing, with adaptive feedback from the data analysis, being used to control and optimize the data acquisition process by the spectrophotometer.

2 The Band Shape and Overlap Problem

A. The Band Shape Problem.—When an oscillator in a condensed medium absorbs energy an absorption band will result as a distribution of intensity over a range of frequencies. The absorption will have a finite width at half-height and a shape function to describe it. There is no reason why the absorption band arising from a molecular transition between the two states should be symmetric, in fact the central moment theorem favours an asymmetric band. Breene has pointed to the limitations of semi-classical theory when applied to the interaction of radiation with matter in not being able to predict absorption and shape functions.[8] The basic theory of line broadening has been discussed by Seshradi and Jones for mainly vibrational spectra.[9]

Nevertheless the band shapes most frequently encountered in absorption profile analysis are the (symmetric) Gaussian, often called the normal curve, and the Lorentzian, or Cauchy, functions. Many successful resolutions of complex absorption band profiles have been reported using these shape functions. One form of the asymmetric Gaussian, in the log-normal form, has also been firmly established.[10,11] When collisional/relaxation processes govern the band broadening mechanism, as in high resolution n.m.r. or vapour phase i.r. spectroscopy, then a Lorentzian-shape function predominates. For relatively rigid systems where the orientations and positions of the interacting species occur essentially during the transition time, the Franck–Condon condition, then Gaussian band shapes dominate the absorption function. Detailed study of the processes that cause bands to have the shapes that they do is worthy of a separate review and we confine ourselves to stating that electronic absorption band shapes are predominantly given by a symmetric, or only slightly asymmetric, Gaussian function.

Ballhausen has recently discussed the theoretical and experimental aspects of the absorption spectra of inorganic complexes in terms of symmetric Gaussian band shapes.[12] For strongly coupled, vibronically allowed, *d–d* transitions of inorganic complexes, the absorption/emission bands have been shown to have a

[8] R. Breene, 'The Shift and Shape of Spectral Lines', Pergamon Press, Oxford, 1961.
[9] R. N. Jones and K. S. Seshradi, *Spectrochim. Acta*, 1963, **19**, 1013.
[10] D. B. Siano, *J. Chem. Educ.*, 1972, **49**, 755.
[11] D. B. Siano and D. E. Metzler, *J. Chem. Phys.*, 1968, **51**, 1856.
[12] C. J. Ballhausen, *Pure Appl. Chem.*, 1975, **44**, 13.

symmetric Gaussian shape function.[13] It has been suggested that both band shape functions can occur in one absorption band associated with a transition, where the overall shape function is a convolution of Gaussian and Lorentzian functions—the Voigt function.[3,14,15] A simple summation of the two band shapes has also been suggested.[1]

The instrument determining the absorption profile has its own slit function and where this value is comparable to the halfwidth of the band being measured the spectrum will be distorted. For research grade u.v.–visible spectrophotometers the slit function is approximated to a simple triangular function and, except for spectra at very low temperatures, almost all absorption bands of condensed systems will be much greater than the band width. Resolution of a band with a halfwidth of y cm^{-1} requires a spectral slitwidth of at least 0.1 y cm^{-1} to achieve more than an indicated value of 99% of the true band height.[16] Good spectrophotometers should be able to achieve a spectral slitwidth of less than 10 cm^{-1}, therefore allowing very good resolution of a band with a halfwidth less than 100 cm^{-1}. Most absorption bands are wider than this and distortion of a spectrum by the function is normally very small and may be disregarded. However, when bands have small halfwidths and the spectrum is recorded under 'difficult' conditions that increase the instrumental slitwidth, such as far-u.v. spectra towards the operating limit, then band distortion must be considered. Various methods have been described to resolve this, such as the Rayleigh–Strutt method and others.[17]

An absorption band profile is a continuous function of wavelength and for purposes of numerical analysis it is taken to be a series of equally spaced frequency values (in cm^{-1}) for which there are corresponding absorbance or absorption coefficient values, *i.e.* a list of n points (ν_i, A_i) or (ν_i, ϵ_i), for $i = 1 \ldots n$. The frequency increments do not *have* to be equispaced for computational purposes but it is usually more convenient if they are. Equispaced wavelength data (in nm) are generally inverted into frequency units, the increments then being unequally spaced. However, if a small moving segment of data is analysed, then the errors involved are small.[6]

Each absorption band has a mode, ν_0 (cm^{-1}), a molar absorption coefficient, ϵ_0 (m^2 mol^{-1}), an area, A (dm^3 m^2 mol^{-1}), and an oscillator strength given by:[18]

$$f = 4.32 \times 10^{-9} 9n/(n^2 + 2)^2 \, A \qquad (1)$$

where n is the refractive index of the medium and A is given by:

$$A = \int_{\text{band}} \epsilon \upsilon \mathrm{d}\upsilon = a_s \epsilon_0 H \qquad (2)$$

where H is the width of the band at half height, $\epsilon_{\frac{1}{2}}$, and a_s is Smakula's con-

[13] H. J. Kaupka, *Chem. Phys. Lett.*, 1977, **47**, 537.
[14] R. B. D. Fraser and E. Suzuki, in 'Spectral Analysis—Methods and Techniques', ed. J. A. Blackburn, Marcel Dekker, New York, 1970.
[15] S. Ganaphty and V. Parthasarathi, *Indian J. Pure Appl. Phys.*, 1977, **15**, 63.
[16] Application Note 16, Cary Instruments, Monrovia, California, U.S.A.
[17] I. R. Hill and D. Steele, *J. Chem. Soc., Faraday Trans.* 2, 1974, **70**, 1233.
[18] A. Rabinowicz, *Rept. Prog. Phys.*, 1939, **7**, 14.

stant. The constant a_s depends upon the shape function of the band; the product $\epsilon_0 H$ gives the area of the 'equivalent triangle' and a_s is the ratio between the area of this triangle and the integrated band shape area with common values of H and ϵ_0. The values of a_s vary from 1.06 for a Gaussian to 1.57 for a Lorentzian shape function.[19]

The Gaussian function has the form, using a standard nomenclature,[20] of:

$$\epsilon(\nu) = \epsilon_0 \exp\left[\frac{-5.545(\nu-\nu_0)^2}{2H^2}\right] \quad (3)$$

whereas the Lorentzian function is given by:

$$\epsilon(\nu) = \epsilon_0 \left[1 + 4\left(\frac{\nu-\nu_0}{H}\right)^2\right]^{-1} \quad (4)$$

An intermediate shape function, the Student-T_3, has been suggested by Morrey for use in band analysis as part of his PEAK program but it has not been applied extensively.[20]

The Gaussian and Lorentzian functions can be compared in several ways, of which the simplest is superposition for common values of ϵ_0, Figure 3a. The Lorentzian function is narrower towards the centre, ν_0, yet does not decrease in intensity into the wings as rapidly as the Gaussian. More analytically, at $\pm 1.5H$ from ν_0 the Lorentzian is approximately $0.1\epsilon_0$ whilst the Gaussian is essentially zero. The functions also have maximum slopes at different points, at $\sim 0.5\epsilon_0$ for the Gaussian and at $\sim 0.75\epsilon_0$ for the Lorentzian. This difference is clearly shown in Figure 3b for the first differentials of the two shape functions which have two such points, by symmetry. The distance between the points is another fundamental property, Δ, the peak-to-peak linewidth. If equations (3) and (4) are differentiated twice, set to zero and solved for $(\nu-\nu)$, we obtain Δ for the Gaussian as $H/\ln 2$ and as $2H/3$ for the Lorentzian.

Important properties of these functions relate to the second and fourth derivatives, plotted for the Gaussian in Figure 4. Both of these derivatives are symmetric about the peak maximum with a decreased 'width', but of opposite sign, at ν_0. The tendency of the bands to 'concentrate' towards ν_0 with successive, even, differentiation plus their distinctive polarities, is used as a decision-making parameter in the analysis of complex absorption band profiles.[20]

Bell and Biggers[21] have used a convolution of the Gaussian with a Lorentzian as a product function to resolve the complex spectra of uranium ions in solution. This form of function has been applied to i.r. spectra by Jones[2] and to Raman spectra by Sundius[3] and a sum function has also been advocated.[2] Increasing the number of variables in a function to fit an absorption profile will automatically increase the 'goodness of fit' of the function to the spectra. Bell and Biggers[21] concluded that uranium ion spectra were better fitted by Gaussian functions with a small Lorentzian perturbation, *i.e.*, a different *weighting* of the functions in the convoluted band shape function, in effect the variation of the weighting

[19] J. J. Markham, *Rev. Mod. Phys.*, 1959, **31**, 956.
[20] J. R. Morrey, *Anal. Chem.*, 1968, **40**, 905.
[21] R. E. Biggers and J. T. Bell, *J. Mol. Spectrosc.*, 1965, **18**, 247.

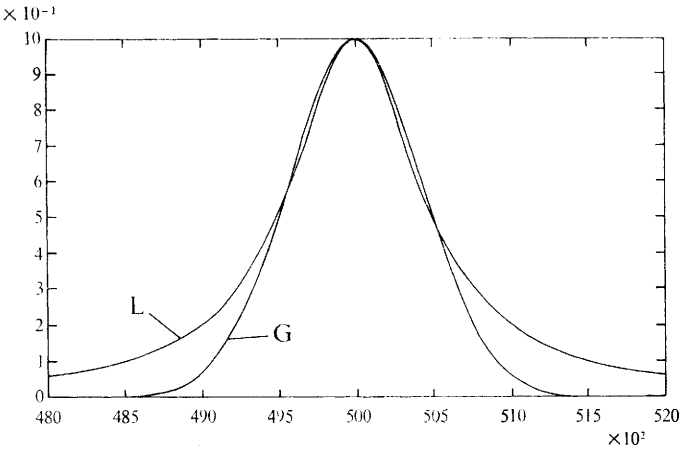

(a)

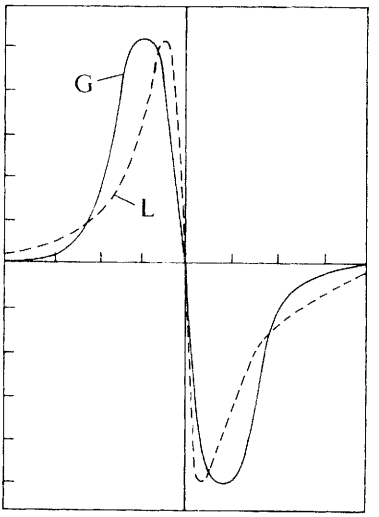

(b)

Figure 3 *Comparison of Gaussian and Lorentzian band shape functions,* (a), *the zero derivative functions both centred on* 50 000 cm^{-1} *with equivalent intensitites,* 1.0, *and equivalent widths at half-height,* 1000 cm^{-1}, *and* (b), *the first derivatives of each shape function as set out above*

parameter, f, for a function of the form.[14] A further elaboration is to use different

$$\epsilon_\upsilon = f\epsilon_0\left[\frac{-5.545(\upsilon-\upsilon_0)^2}{2H^2}\right] + (1-f)\epsilon_0\left[1 + 4\left(\frac{\upsilon-\upsilon_0}{H}^2\right)\right]^{-1} \quad (5)$$

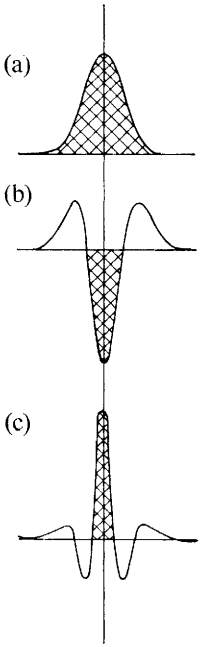

Figure 4 *Zero* (a), *second* (b), *and fourth* (c) *derivatives of a Gaussian band shape*

values of H for each term in equation (7).[14] Where the function is used in a linear combination of such shapes, the values of f may either be the same for all bands or assumed to be different for each band. A combination of variable H and f parameters could be very powerful and must be used with great care. The variation of f poses some interesting chemical–physical questions of interpretation.

The moments of the shape function about the mean are useful. The nth moment of a curve μ_n, is defined by:[22]

$$\mu_n = A\int_{\text{band}}\epsilon(\upsilon)(\upsilon-\upsilon_0)^n d\upsilon \tag{6}$$

where ν_0 is the mean, defined by:

$$\upsilon_0 = A^{-1}\int_{\text{band}}\epsilon(\upsilon)\,\upsilon^n d\upsilon \tag{7}$$

The odd moments of both shape functions disappear by symmetry and the second and higher moments of the Lorentzian are infinite. The Gaussian moments are $\mu_2 = \Delta^2$, $\mu_4 = 3\Delta^4$, and $\mu_6 = 5\Delta^6$, *etc.* A band shape function will be completely characterized by specifying all of the moments about the mean and

[22] J. H. Van Vleck, *Phys. Rev.*, 1948, **74**, 1168.

can be reconstructed using Edgewood's formula.[23] The higher moments will be affected by experimental error in the 'wings' of the band where it is most likely to be overlapped. Band moment analysis is particularly important for asymmetric shape functions, where odd moments do not disappear by symmetry.

Siano has shown that experimental data rarely conforms to a normal distribution.[10] A fundamental reason is that a normal (Gaussian) distribution is symmetric and that if any observable quantity takes on a value greater than twice the mean, then it must be able to take on negative values as well. But spectroscopic values are always positive with respect to the ordinate, the Gaussian is therefore inappropriate and the distribution is usually positively skewed. Moreover, a symmetric function has little underlying theoretical justification for both the central moment theorem and the configuration co-ordinate approach lead to an asymmetric absorption profile.[10]

Pearson's method gives further insight into the symmetry of an absorption band.[20] Normalized third and fourth moments are given by

$$\beta_1 = \mu_3^2/\mu_2^3 \tag{8}$$

$$\beta_2 = \mu_4/\mu_2^2 \tag{9}$$

where μ_n is defined by equation 6 and can be calculated from the experimental data. An analytical expression is obtained that best fits the data from a family of Pearson's curves associated with the calculated values of β_1 and β_2. This method has been applied to pyridine derivatives and Figure 5 shows their spectra to be quite clearly asymmetric. Figure 5 also illustrates the difficulty of fitting two types of asymmetric band shapes to the experimental absorption profiles.[11] The most common asymmetric shape functions are the two halfwidth Gaussian (Fechner's distribution) and the log-normal. For comparison the functions have been constrained to go through ϵ_0 and $\epsilon_0/2$, as defined in the inset to Figure 5. The log-normal function fits the data very well, whereas the two halfwidth Gaussian consistently underestimates data on the high energy side and overestimates the data on the low energy side. For the spectra of pyridoxal in 0.1 M-HCl in Figure 5, four curves were extrapolated into the region of overlap and the moments calculated. The results give $1.1 < \gamma < 2.0$ where γ is defined by:

$$\gamma = (\beta_2 - 3)/\beta_1 \tag{10}$$

and β_1, β_2 are defined in equations (8) and (9). The corresponding analytical expression lies in Pearson's type VI curve, bounded by the types III and IV. It would be better if further criteria could be used to distinguish between these alternatives. The log-normal distribution lies completely within the Pearson type VI curve region with $\gamma = 1.80$.[24] Because it has other attractive features, such as ease of manipulation, Siano and Metzler[11] have used this type of distribution

[23] H. Cramer, 'Mathematical Methods of Statistics', Princeton University Press, Princeton, N.J., 1954; G. Wetherill, 'Elementary Statistical Methods', Methuen, 1967.

[24] K. Pearson, *Phil. Trans.*, 1912, **216**, 456; W. P. Elderton, 'Frequency Curves and Correlation', C. and E. Layton, London, 1927.

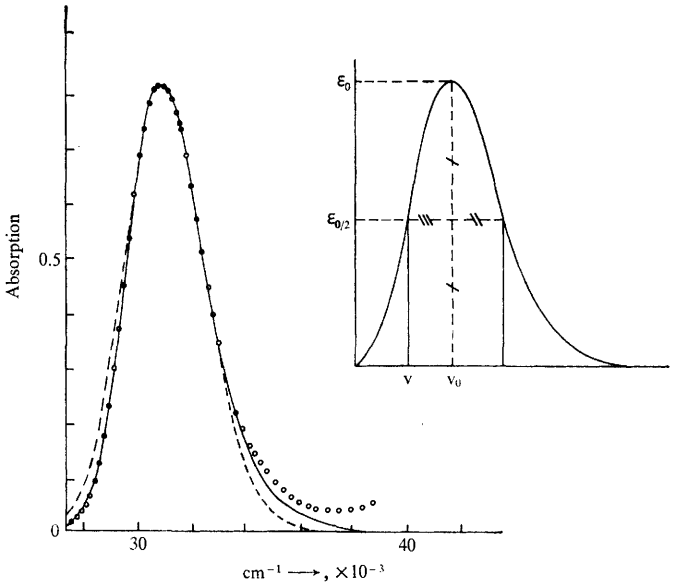

Figure 5 *Comparison of the log-normal (full line) and two halfwidths Gaussian (broken line) and absorption spectra, experimental values denoted by (●) for 3-hydroxypiridine. Inset the log-normal band shape with positive skewness showing the definition of the parameters*
(Reproduced by permission from *J. Chem. Phys.*, 1968, **51**, 1856)

extensively. The log-normal function fits the spectra of the other pyridine derivatives very well, Figure 5, not only on the low energy side of the absorption bands but also on the upper two thirds of the high energy edge. The fit is worse at higher wave numbers because of a further band. Another example is given by Figure 6 where a spectrum is analysed as the sum of six log-normal shape functions.[4] The fit to the profiles is very good on the low energy edge and at the most difficult points, the peak and valley areas. The log-normal distribution has the form:

$$\epsilon(v) = \frac{\epsilon ab}{(v-a)} \exp \frac{(-c^2)}{2} \exp \frac{-1}{2c^2} \left[\ln \frac{v-a}{b}\right]^2 ; v > a \tag{11}$$

$$\text{and } \epsilon(v) = 0 ; v < a \tag{12}$$

where a, b, and c are related to v_0, H, and ρ by:

$$a = v_0 - H[\rho(\rho^2-1)] \tag{13}$$

$$b = H[\rho/(\rho^2-1)]\exp c^2 \tag{14}$$

$$c = \ln \rho/(2\ln 2)^{\frac{1}{2}} \tag{15}$$

The area under the log-normal curve is given by equation 2, where Smakula's constant, a_s, now varies with ρ, from 1.06 to 1.09 for ρ varying between 1.0 and

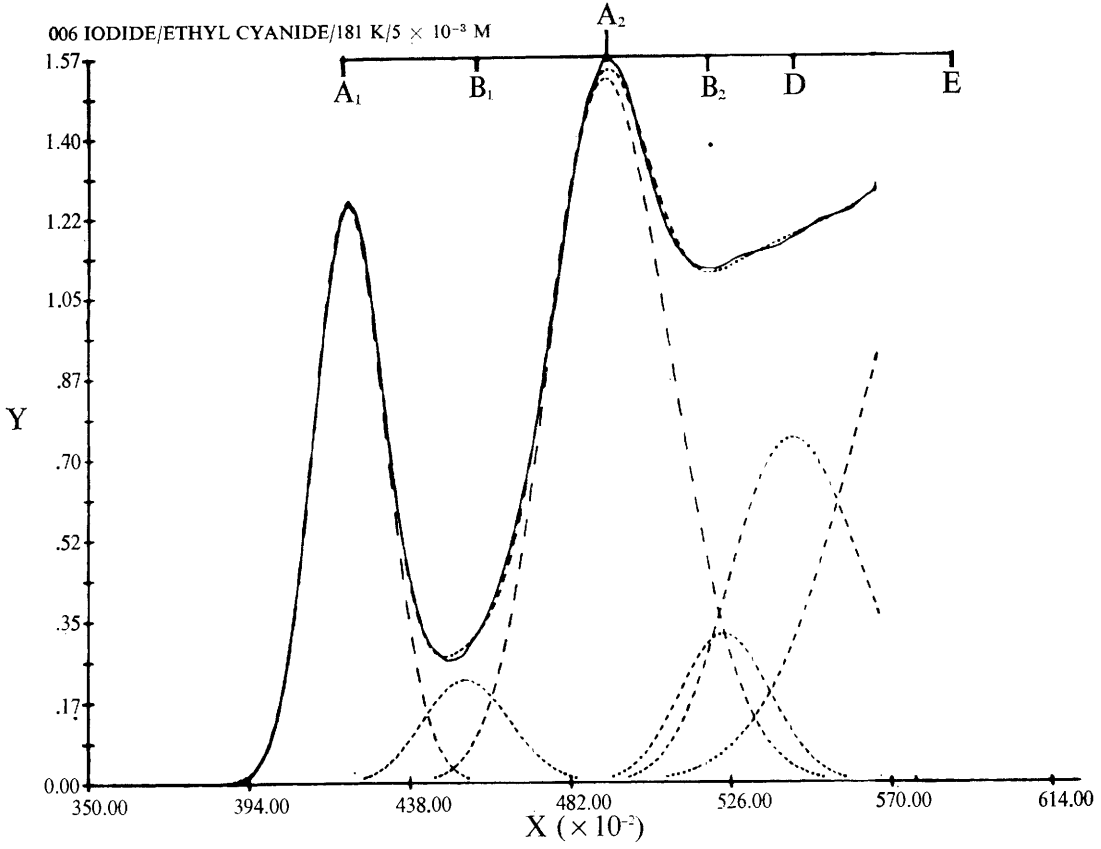

Figure 6 *Resolution of the absorption spectrum of tetramethylammonium iodide at* 5 × 10^{-3} mol dm^{-3} *in propionitrile at* 181 K, *using log-normal band shape for each*
(Reproduced from *J. Chem. Soc., Faraday Trans.* 1, 1977, **73**, 1003)

1.5.[21] Many properties of the log-normal are obtained from the properties of the Gaussian, as it reduces asymptotically to the Gaussian form as $c \rightarrow 0$ and $\rho \rightarrow 1.0$. The asymmetry, ρ, is defined as $(\nu_2 - \nu_0)/(\nu_0 - \nu_1)$, Figure 5 (inset). The function must be manipulated carefully as the limiting condition of $\rho \rightarrow 1.0$ is approached, for the classical computing error of dividing by zero is very readily committed. An empirical approach is to fit an absorption band with a function of the form[14]

$$\epsilon(\upsilon) = \epsilon_0 \, 1 + [2a^2 - 1][2\,(\upsilon - \upsilon_0)/H]^2 - 1/a^2 \qquad (16)$$

where a varies between 0 and $2^{\frac{1}{2}}$. Equation (16) reduces to the Gaussian form when $a = 0$ and to the Lorentzian form when $a = 1$. When $a > 2^{\frac{1}{2}}$, the area beneath the curve becomes infinite.

Although there are many shape functions, for utility only three functions have been used extensively for electronic absorption spectra, namely the Gaussian (normal), the log-normal, and, occasionally, the convolution of a major Gaussian with a minor Lorentzian as one form of the Voigt function.

B. The Band Overlap Problem.—When two, identical, well separated bands with Gaussian shape functions are moved towards each other such that they increasingly overlap, then their separate identities are slowly lost, Figure 7a. The condition that only one overall pseudo-Gaussian band shape remains occurs when the peak separation is a small multiple of the half bandwidth. When the two bands do not have the same intensity, but the same halfwidth, the overall effect of decreasing the separation between these bands is shown in Figures 7b and 7c, where the ratio of intensities is first 2:1 and then 5:1. This effect was first demonstrated by Vandenbelt and Henrich[25] and is drawn here from computer generated profiles.

From these examples, without even considering the additional possibility of the absorption bands having different half bandwidths, it can be seen that even a reasonable guess of peak maxima cannot be obtained in most of the cases shown in Figure 7. The need for analytical methods to determine true peak positions of components is made by Figure 7 for only two bands; for real situations, where there are usually more than two components, the need for analytical methods is overwhelming.

3 Methods of Analysis

Computer methods resolving electronic absorption band profiles are applied at several related strategic levels of analysis. Some methods use one level, others use two levels, and these are broadly defined as:

(i) an initial, unoptimized analysis, which operates on the original data without previous indication of band parameters;

(ii) optimization of the band parameters obtained from (i) by the use of convergence techniques, described in Section 4.

A method that operates directly on the data in (i) will give band parameters

[25] J. M. Vandenbelt and C. Henrich, *J. Appl. Spectrosc.*, 1953, **7**, 171.

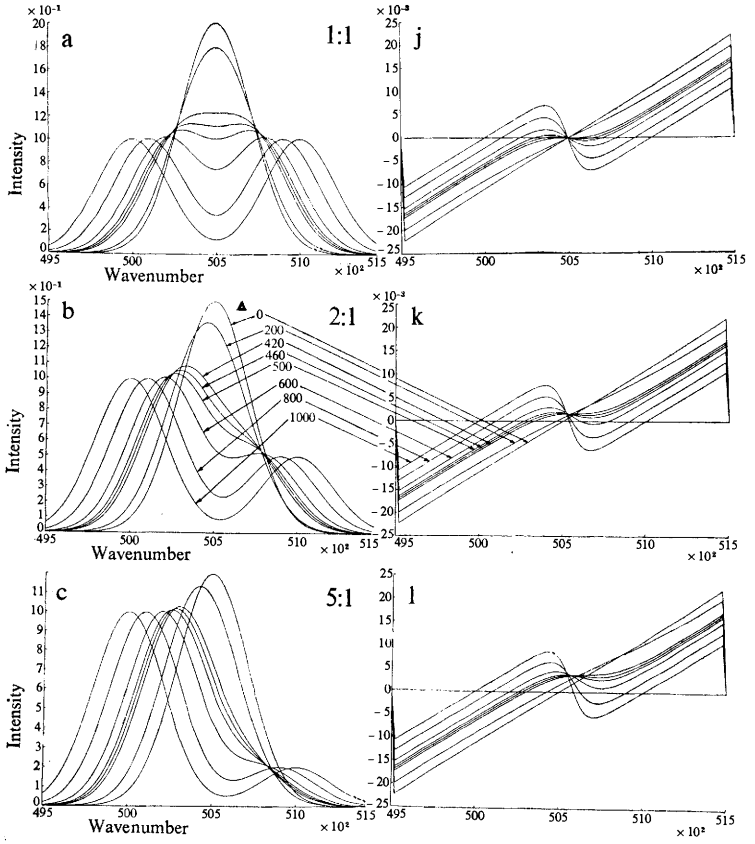

Figure 7 *The effect of gradually increasing band overlap on* (a) *two identical bands with an initial separation of* 1000 cm^{-1} *between* ν_{max} *and a half bandwidth of* 500 cm^{-1}, *and* (b) *two bands with an intensity ratio of* 2:1, *separation of* 1000 cm^{-1} *and half bandwidths of* 500 cm^{-1}, (c) *two bands intensity ratio* 5:1, *separation of* 1000 cm^{-1} *and half bandwidth of* 500 cm^{-1}
(B. E. Barker and M. F. Fox, to be published)

that are inaccurate owing to the presence of other, closely overlapped, bands. Reconstruction of the band profile shows that substantial inaccuracies exist and that the analysis is only a reasonable approximation to the original band profile. The 'fit' of the analysed profile to the original is improved by the second strategic level that uses various techniques to reduce these discrepancies, Section 4.

The first level of analysis may be divided into three subcategories, namely inspection, analogue, and digital methods. Indeed with experience and intuition, quite reasonable estimates of band parameters can be made by inspection. These are used as initial values for iterative convergence techniques[14] and represent a

useful approach *only* if the profile is uncomplicated. An analogue method is used in the Du Pont Curve Resolver, Figure 8. The spectrum to be resolved is

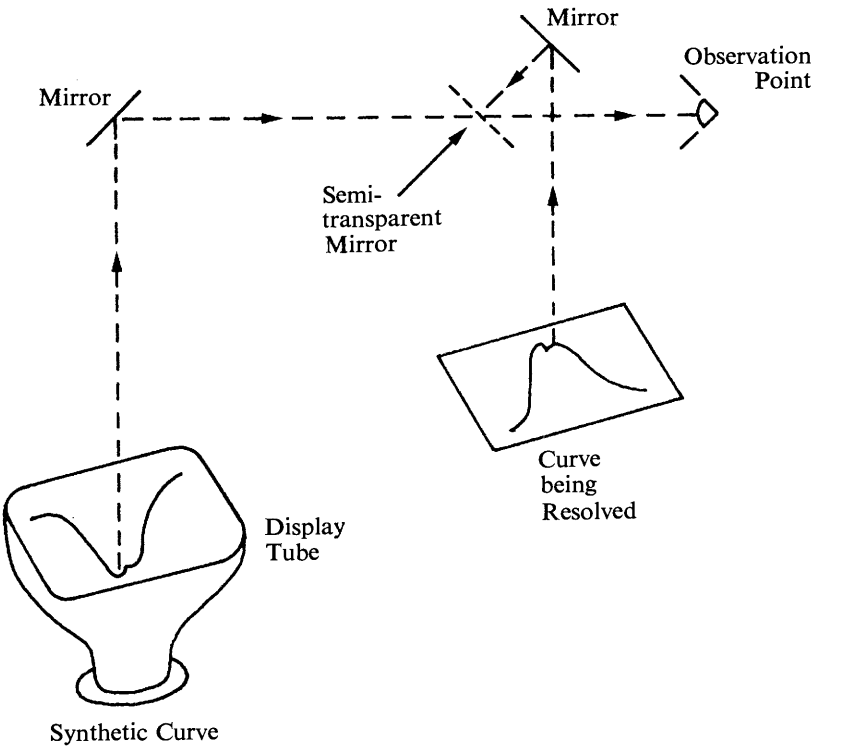

Figure 8 *The optical system of the DuPont Curve Resolver*
(Reproduced by permission from Dupont Co. Ltd.)

placed on the bench of the apparatus and is presented to the operator as a laterally correct image by double reflection. A high intensity cathode ray tube projects a synthesized spectrum through the second (half silvered) mirror such that it is directly superimposed upon the image of the original spectrum. The synthesized profile is the sum of individual band shapes, each obtained from a central shape function generator. As this is an analogue method, the shape function is set by adjusting a single profile to a standard curve, *e.g.* Gaussian, Lorentzian, or Voigt shapes. Up to twelve channels are possible with each channel representing a band shape function whose position (ν_0), height (ϵ_0), and width, (H), may be varied individually. The skewness (ρ) may be introduced as an additional parameter using a different type of channel controller. A complex absorption profile may be synthesized and fitted to the spectrum by using between two and twelve channels. Further features include an integrating meter which

can give the percentage area of each individual band relative to the whole profile and also an X–Y plotter that can plot the overall profile, the individual component bands, and the baseline.

Such a fascinating and absorbing apparatus can readily submerge the chemical aspects of the problem. We state two rules at this stage which should help to keep the problem in chemical perspective.

Rule 1: The minimum number of component bands must be used consistent with a 'good' resolution that leaves the residual errors at a level consistent with noise—a restatement of Occam's razor.

Rule 2: The number of component bands used in a resolution must relate to a chemical and physical model for the system studied.

The Du Pont resolver has been used to analyse several systems, *e.g.* Gaussian band shapes in Raman spectra,[26] far-u.v. halide absorption spectra in solution,[27] and a particularly interesting application in the resolution of both the u.v. absorption and circular dichroism spectra of nucleotides in solution.[28] For the last application the synthesized band shapes were used in both positive and negative absorbance modes to synthesize the extremely complex circular dichroism spectra, Figure 9. Used with care, discretion, and within the framework of several possible chemical models for a system, the Du Pont analogue system is a powerful tool for the resolution of overlapping absorption bands.

A similar method, but in a digital form, is to generate band shape functions on a graphical visual display computer terminal on which the experimental spectrum is displayed. Through a joystick control or light pen[29,30] an overall absorption profile is synthesized from individual band components by a process of trial and error that can be made to fit the original absorption profile using either a 'refresh graphics' or storage tube method.

These methods are 'driven' by the operator and can be time-consuming. The results are subject to a level of error that can make a study of band parameters as a function of temperature for resolved absorption bands to be so scattered as to be meaningless. On the other hand, these methods are relatively simple and can give a good first estimate of band parameters. There is, however, an element of subjectivity in obtaining a 'good' resolution. The values obtained may be either accepted as first approximations or used as inputs for minimization convergence procedures at the next strategic level, Section 4.

Digital numerical analysis methods offer the possibility of obtaining band parameters directly from a spectrum represented as a set of co-ordinates. The two main methods used are those which either differentiate the profile directly and those which rely on a least squares fitting procedure to fit a polynomial to the absorption profile.

[26] G. E. Walrafen, in 'Water—A Comprehensive Treatise', Vol. I, ed. F. Franks, Plenum, New York, 1972.
[27] B. E. Barker, M. F. Fox, and E. Hayon, *J. Chem. Soc., Faraday Trans.* 1, 1978, **74**, 1776.
[28] D. W. Urry, in 'Spectroscopic Approaches to Biomolecular Conformation', ed. D. W. Urry, American Medical Association, Chicago, 1970, Chapter 3.
[29] Leicester Polytechnic Deconvolution Programme, 1980, available on request.
[30] P. Gans, *Computers and Chemistry*, 1977, **1**, 29.

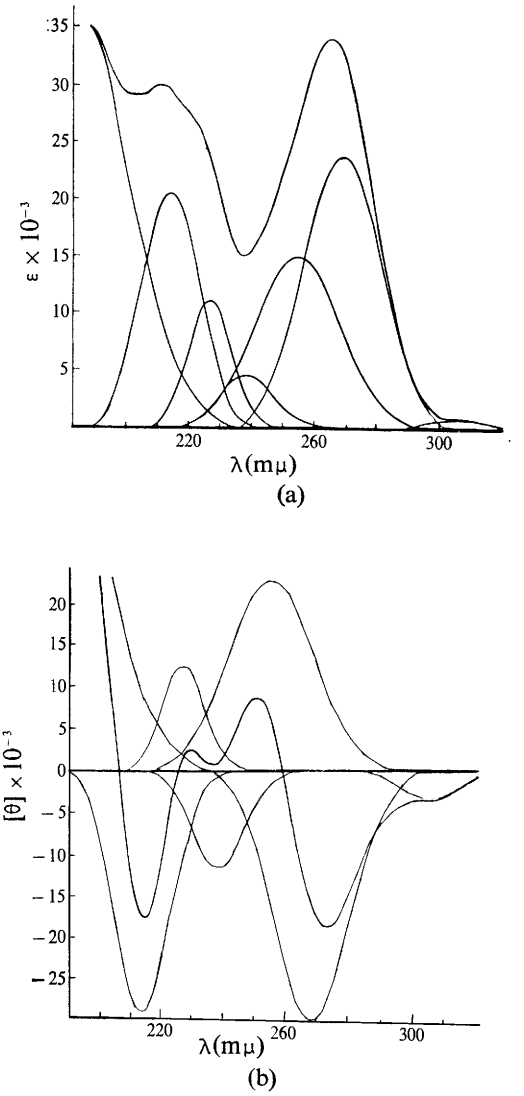

Figure 9 (a) *Resolved absorption spectra of stacked flavin adenine dinucleotide: these resolved bands are used to analyse the circular dichroism spectrum of the same compound,* (b)

(Reproduced by permission from 'Spectroscopic Approaches to Biomolecular Conformation', American Medical Association, Chicago, 1970, Ch. 3)

A. Differential Methods.—Methods using properties of the first or higher differentials of the absorption profile fall into two groups. The first group is

exemplified by the PEAK program of Morrey[20] and the work of Butler and Hopkins.[31] These programs act on the whole absorption profile and are independent of the operator once the procedure is initiated. The second type of method, LOGDIFF,[6] is an interactive method dependent upon the judgement of the operator and acts upon the component bands of absorption profiles in a sequential manner.

Morrey's PEAK program is examined as an example of the first type of differential analysis. Although we have demonstrated the preference for Gaussian band shape functions in the analysis of electronic absorption band profiles, the PEAK program may be applied to Gaussian, Lorentzian, and the (intermediate) Student-T_3 functions.

The spectroscopic data is defined as a set of co-ordinates for the absorption (ϵ) and equi-spaced wavelength (λ) or wavenumber (ν) axes. A quartic equation is fitted to a segment of the data and v_j is defined as a position relative to a position v_k spanned by the data segment. Then, if we let;

$$d\epsilon_j/dv_j = \sum_{i=1}^{5} C_i\,(i-1)v_j^{(i-2)} \tag{17}$$

$$d^2\epsilon_j/dv_j^2 = \sum_{i=1}^{5} C_i\,(i-1)(i-2)v_j^{(i-3)} \tag{18}$$

$$d^3\epsilon_j/dv_j^3 = \sum_{i=1}^{5} C_i\,(i-1)(i-2)(i-3)v_j^{(i-4)} \tag{19}$$

$$d^4\epsilon_j/dv_j^4 = \sum_{i=1}^{5} C_i\,(i-1)(i-2)(i-3)(i-4)v_j^{(i-5)} = 4!\,C_5 \tag{20}$$

At the peak positions, the conditions apply that are illustrated in Figure 3 and can be written as:

$$d^2\epsilon_j/dv^2_j < 0 \tag{21}$$

$$d^3\epsilon_j/dv^3_j = 0 \tag{22}$$

$$d^4\epsilon_j/dv_j^4 > 0 \tag{23}$$

There are other conditions that define a peak but the higher derivatives will reduce the relevant range of v_j and increase the accuracy of resolution by reducing the effects of overlapping bands *provided that the data have a very low noise component.*

The analysis proceeds by evaluating C_5 for the data increment and if it is positive, then zero values for $d^3\epsilon_j/dv_j^3$ within the increment are found by:

$$v_0 = v_k + v_0 \tag{24}$$

$$\text{where } v_0 = \frac{-3!C_4}{4!C_5} \tag{25}$$

If such values of ν_0 exist, then $d^2\epsilon_j/d\nu_j^2(\nu_0)$ is calculated to determine whether it is negative by:

[31] W. L. Butler and D. W. Hopkins, *Photochem. Photobiol.*, 1970, **12**, 439, 451.

$$d^2\epsilon_j/dv_j^2 = 2C_3 + 6C_4v_0 + 12C_5v_0^2 \quad (26)$$

in which case v_0 is a peak position.

The data segment to which the quartic equation is fitted is then moved on by adding a new 'front' absorbance value and dropping the 'rear' one. The computation is then repeated and the process continued until the whole absorbance profile has been traversed. A data segment spanning an absorption band peak will give several values of v_0, the number of values depending upon the length of the data segment relative to the peak width. Adjustment of the data increment to be considerably less than the minimum half bandwidth present is crucial for successful application of the PEAK program. A final value for v_0 is obtained using the previous value of v_0 extrapolated from the data point nearest to it. v_0 is obtained using a quartic fit to the data and thus the band shape functions are not considered. The halfwidths and intensities of the band at v_0 are calculated using the initial polynomial coefficients, C_i, and the appropriate relationship for the three band shape functions.

The PEAK program has been found to be very sensitive to the level of noise present, due mainly to the use of higher differentials which accentuate the effect of noise. Minimization of the noise component and careful adjustment of the data increment and data segment length parameters can transform the PEAK program from generating meaningless numbers to meaningful results.

The PEAK program is unusually thorough in its exploration of errors caused by adjacent peaks and the limits of peak detection. General sources of error are identified. First the inaccuracies that arise from fitting a polynomial to a segment of an absorption profile. Errors from this source are found to be considerably less than those from the second source, which arises from bias errors introduced by two adjacent and overlapping peaks. The effect of adjacent peaks on the errors in determining v_0 was analysed to show that, given the progression of band overlap in Figure 7, one of those peaks will not be found under extremal conditions. Indeed, under certain conditions, an illusion of a third peak can be generated in the analysis of two overlapping bands and the parameters for this condition have been set out as a nomogram. The PEAK program can be applied to both wavelength and wavenumber data, the energy asymmetry of wavelength axes probably being too small for a limited data segment to introduce significant additional error.

The attention given to the limits of the resolution method in the PEAK program is also a feature of another differential method, LOGDIFF.[6] Both least squares fitting and differential methods are used and the method is first examined for a single Gaussian—the method is only applicable to Gaussian band shapes.

Thus for a single Gaussian absorption band centred at v_0 with maximum intensity ϵ_0 and width at half height, H, then H is related to the standard deviation S of the Gaussian distribution function by:

$$H = 2S(2\ln 2)^{\frac{1}{2}} \quad (27)$$

Then $$\Phi(v) = \epsilon_0 \exp -\tfrac{1}{2}\left(\frac{v - v_0}{S}\right)^2 \quad (28)$$

and $\psi(\nu)$ is defined by:

$$\psi(v) = \mathrm{d}(-\ln\Phi)/\mathrm{d}v \tag{29}$$

which satisfies

$$\psi(v) = (v - v_0)/S^2 \tag{30}$$

In a region where the wavenumber spectrum consists of a single Gaussian peak, the quantity $\psi(\nu)$ is linear in ν with a slope equal to S^{-2} and $\psi(0) = \nu_0$. This condition is only true for a composite absorption profile in which there are regions where one band dominates all of the other bands. The LOGDIFF methods proceed by transforming the original spectrum Figure 10a, through equation (29), the transformed data are plotted and a linear portion (of positive gradient) selected using the crosswires (+), Figure 10b.The linear portion between the crosswires may be examined more closely, Figure 10c, and if it is found to be satisfactory, the values of S (hence H) and ν_0 are estimated from this segment and ϵ estimated from:

$$\epsilon = \phi(v)e + \tfrac{1}{2}\left(\frac{v - v_0}{S}\right)^2 \tag{31}$$

Least mean squares and minimum curvature techniques are used to optimize the calculation of ν_0 and S. Now that all of the band parameters are known, it is possible to remove the band from the overall absorption envelope, Figure 10d. In this way, 'band peeling' will reveal smaller bands which are hidden by being overlapped by much larger bands. Several attempts may be made to remove a peak before an acceptable solution is found. The procedure moves on to remove the next peak, Figures 10d—f. The accuracy of the band resolution is reflected in the quality of the baseline remaining. The parameters of the small band revealed in Figure 10f are obtained by the transform shown in Figure 10g and calculation of the slope at $\sim 45\,000$ cm^{-1}.

As bands became more overlapped, as in the high energy side of Figure 10f, then an accurate deconvolution cannot be obtained. The limitations of resolution for the LOGDIFF have been presented in a graphical manner that relates the relative bandwidths, band peak separation, and absorbance maximum ratio for the two bands considered.[6]

Comparison of the results obtained using the LOGDIFF method with other techniques, such as the analogue curve resolver and geometrical construction methods, show that LOGDIFF gives more consistent results for a set of spectra recorded over a range of temperature. LOGDIFF has the advantage of dealing with each peak individually, together with the derivative of peak parameters from a least mean squares approach. On the other hand, LOGDIFF is not as effective as the iterative least mean squares method of fitting a series of absorption curves to an absorption profile. It is an effective method of preliminary analysis for an absorption profile in either its operator-driven or automatic[32] form. Where a very high quality of fit is not required for an analysis,

[32] B. E. Barker and M. F. Fox, to be published.

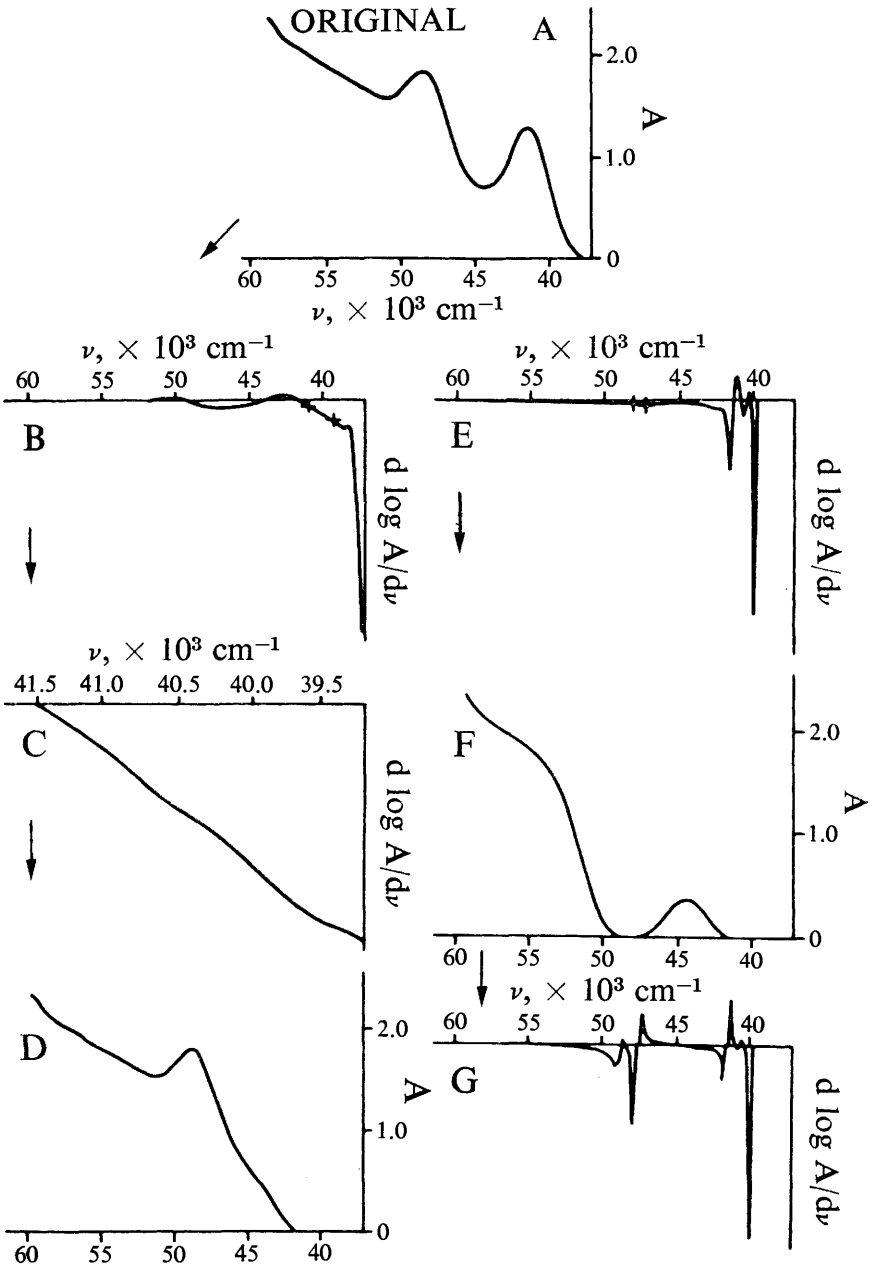

Figure 10 *Visual display of data for* 5×10^{-3} mol dm^{-3} *tetra-n-butylammonium iodide in triethyl phosphase at* 253 K. (a) *Experimentally obtained absorption spectrum,* Φ. (b) d log A/dν *of* (a) *plotted against* ν, (ψ), *showing cross-wires controlled by joystick.* (c) *Expansion of* ψ *between the crosswires of* (b) *above showing region of interest for peak removal.* (d) Φ, *i.e.* (a) *with the first peak removed. This spectrum is then made an original spectrum, as* Φ'. (e) d log A/dν *of* (d), ψ', *showing linear region denoted by crosswires.* (f) (a) *with second peak removed. The remaining spectrum is then again treated as an original data set,* Φ''. (g) d Log A/dν *for* (f) *giving the band parameter of the small band at approx.* 44 000 cm^{-1}

(Reproduced from *J. Chem. Soc., Faraday Trans.* 1, 1976, **72,** 1990)

LOGDIFF is sufficient to obtain the parameters of bands contributing to an absorption profile.

B. Least Squares Methods.—The convolution least squares method was introduced by Savitsky and Golay for curve fitting, data smoothing, and peak finding.[33] The method has been extended by Johnson and Harmony[34] and proceeds as follows:

The nth degree polynomial which best fits (in a least squares sense) a set of $2m + 1(e_i,\nu_i)$ co-ordinates is given by:

$$\epsilon_{in_0} = b_{n_0} + b_{n_1} i + b_{n_2} i^2 + \ldots b_{nn}\, i_n = \sum_{k=0}^{n} b_{nk} i_k \tag{32}$$

$$\text{where } b_{nk} = \frac{1}{k!} \frac{\sum_{i=-m}^{+m} C_i(n,k,m)_i}{\Delta^k N_{nkm}} \tag{33}$$

The wavelength/wavenumber values of the data are equally spaced with an interval Δ and a new variable, i, is defined by:

$$i = \frac{\upsilon + \delta}{\Delta} \tag{34}$$

The purpose of the method is to find the value of the wavenumber/wavelength or the maximum of the symmetric absorption band with a Gaussian or Lorentzian shape function. Neither of these functions can be fitted exactly by a polynomial, but then most absorption bands do not follow the shape functions exactly. However, a second degree function is a suitable approximation for locating the maxima of the band, but necessarily introduces error. The error can be decreased by several adjustments such as using a polynomial which gives a better fit (such as a third degree polynomial for a slightly asymmetric band) or reducing the data increment such that the intervals are small compared to the natural half bandwidth of the function, or the development of suitable correction terms which are applied after the fitting procedure.

Of these alternatives, the first leads to an expanded computation because additional b_{nk} terms must be evaluated. The second alternative leads to the inclusion of a significantly increased number of data points, again leading to increased computation. The third alternative considers the non-random, non-experimental error in finding the peak maximum to be a function of four or more parameters, first, the degree of the fitted polynomial, second, the number of data points, third, the true functional form of the data, and fourth, a parameter ν_R which describes the position of the central data point relative to the true maximum, ν_{max}, of the function described by the data. A factor[34] was derived for the correction of ν_{max} (apparent) to ν_{max} (actual) for both Gaussian and Lorentzian functions and shown to be beneficial in reducing errors.

[33] A. Savitsky and M. J. E. Golay, *Anal. Chem.*, 1964, **36**, 1627.
[34] L. J. Johnson and M. D. Harmony, *Anal. Chem.*, 1973, **45**, 1494

However, as much as these refinements improve the original approach of Savitsky and Golay,[33] there remain fundamental causes of error that apply to all of these analytical methods. First, there is the assumption of a symmetric band shape (or summation/product of Gaussian/Lorentzian functions) which will ideally fit an absorption band profile. It is a moot point whether the increase in the number of parameters introduced by using two symmetric, but different, band shape functions that can further reduce the error between a synthetic and an original profile will actually provide any further chemical insight. To increase the complexity of any function being fitted to a profile can always increase the 'fit' of that function to the profile simply because the number of degrees of freedom in the fitting function has been increased. The less complex variant of introducing skewness, *via* the log-normal function, has been preferred by others. An approach using a mixture of asymmetric band *shapes* does not appear to have been reported. To decide whether one form of band shape (or collection of band shapes) has significantly decreased error, an analysis of variance as described by Hamilton[35] is required; this has not been done.

We know that absorption bands do not follow a given band shape exactly, particularly in the 'wings', sufficient to upset precise, unoptimized, analytical methods. Furthermore the effect of overlapping bands on the estimation or analytical determination of individual band parameters is considerable and is not readily corrected at this stage. Therefore, an optimization procedure is necessary to fit the synthetic profile to the experimental absorption band by complex and subtle adjustments of the initial parameters obtained using the previously described procedures.

4 Optimization Methods

Reconstruction of the synthetic absorption profile and comparison with experiment often shows substantial discrepancies, the most obvious regions generally being the peak and valley regions of the profile. The purpose of optimization methods, in colloquial terms, is to 'shrink-wrap' the synthetic profile on to the experimental profile. To achieve this end, we must first define a measure of the 'goodness of fit' between the two profiles that can be used as a criterion, and second, we review the methods used to maximize the 'fit'. The main methods that have been applied to the deconvolution of *electronic* band profiles are described here. Gans has written an excellent review of data fitting in chemical problems using numerical methods.[36]

A. The Criterion of 'fit'.—The least squares criterion is regarded as the best, but not the only choice for measuring the 'goodness of fit'. It is the easiest to manipulate but the proof of its ideal suitability lies with the assumption that the main cause of error between the function and the data lies with the latter. Given the accuracy of u.v.–visible spectrophotometers and the reservations described

[35] W. C. Hamilton, *Acta Cryst.*, 1965, **18**, 502.
[36] P. Gans, *Co-ord. Chem. Rev.*, 1976, **19**, 99.

previously over the suitability of band shape functions, the assumption may not be valid.

Legendre introduced the least squares method in 1806 to fit discrete experimental data to a continuous function, generally for the linear (trend line) case. The parameters of the continuous function are assumed to be linear, whereas the band shape functions discussed previously are non-linear in their parameters. Therefore they must be reduced to an approximately linear form through the application of Taylor's theorem and the best fit found by iteration. The procedure sets out to find particular values of the band parameters p_i, p_1, p_2, p_3, which give an optimum fit of the function $\epsilon(\nu, p_j)$ to a set of discrete data points (ϵ_i,ν_i) in the sense of minimizing the unweighted sum of the squares of the deviations, given by:

$$S = \sum \left[\epsilon_i(\upsilon_i,p_j) - \epsilon_i\right]^2 \tag{35}$$

and it is this term that is minimized in the GSAN program of Schwarz.[33] Other workers prefer to use the root-mean-square deviation between the synthetic and observed profiles, δ_{rms}, sometimes using a weighting function, W_i,[14] as:

$$\delta_{\text{rms}} = \left\{ \frac{\sum_i^n W_i[\epsilon_i(\upsilon_i,p_j) - \epsilon_i]^2}{\sum_{i=1}^n W_1} \right\}^{1/2} \tag{36}$$

In almost all applications in electronic spectroscopy the value of W_i is taken or implicitly assumed to be unity and equation (36) then reduces to the square root of equation (35).

In conventional least squares methods the function $\epsilon_i(\nu_i,p_j)$ is a polynomial in ν with coefficients p_j. Using this function leads to a set of simultaneous algebraic (normal) equations. Solutions to these equations directly give the set of least squares parameters, p_j. However, a function which is a summation of Gaussian components gives a set of simultaneous equations which are non-linear in the unknown p_j's and one incapable of exact solution. Where we have good estimates of the p_j's, the problem of not being able to obtain exact solutions for the p_j's is resolved by the use of the stratagem that there is an exact solution, p_j^0, and that the inexact solution, p_j, is related to the exact solution by Δp_j, as

$$p_j = p + \Delta p_j \tag{37}$$

S can now be written as:

$$S = \sum_i \left[\epsilon_i (\upsilon_i \;_j + \Delta p_j) - \epsilon_i\right]^2 \tag{38}$$

As we have good estimates for p_j^0, obtained by the previous strategic level of analysis, Δp_j will be small and ϵ_i can be approximated by a truncated Taylor series expansion about p_j^0,

$$\epsilon_i(\upsilon_i,p_j^0 + p_j) \approx \epsilon_i(\upsilon_i,p^0) + \Sigma_j (\epsilon'_{ij}) \Delta p_j \tag{39}$$

The partial derivatives ϵ'_{ij}, equal to $(\partial\epsilon/\partial p_j)$ are those for ϵ with respect to the parameters p_j and are found at each ν_i with p_j set at p^0. S is now given by:

$$S = \Sigma_i [\epsilon(\nu_i, p^0) + \epsilon_j(\epsilon'_j)\, \Delta p_j - \epsilon_i] = \text{minimum} \qquad (40)$$

If there are J component bands in the spectrum then each $(\partial\epsilon/\partial\Delta p_j) = 0$ gives a set of $3J$ normal equations in $3J$ unknowns. In matrix notation, this set can be written concisely as:

$$a.\Delta p = b \qquad (41)$$

where the elements of the a and b are, respectively:

$$a_k = \Sigma_i(\epsilon'_{ik})(\epsilon'_i) \qquad (42)$$

$$b_k = \Sigma_i(\epsilon'_{ik})[\epsilon_i - \epsilon\, \nu_i, p_k] \qquad (43)$$

where j, k, and i refer to component peaks. Matrix inversion gives the vectors Δp and gives the set of corrections Δp_i which give a better set of p_j^0 for the next iteration. The exercise is repeated until the calculated value of S falls below a preset value.

B. Convergence.—Writing a convergence program has been extremely difficult in the past. It can be seen now that the success of the convergence depends critically on the quality of the initial estimates of the band parameters. If they are poor the value of S may either diverge on iteration, as Schwarz has pointed out,[37] or a false minimum may be obtained. On the other hand, if the estimates have been obtained either from an experienced estimate or from a lower level of analysis as described in previous sections, then they are reasonably close to the best-fitted estimates.

Three methods have been incorporated into the Leicester Polytechnic Spectrum Analysis program,[29] namely the line of steepest descent, the Newton–Raphson, and the Gauss–Newton methods. Each of these is iterative in that they start with a vector p_n and calculate from this a vector p_{n+1} which is an improvement. Using as a general form:

$$p_{n+1} = p_a \frac{-SA\, g'(p_n)}{|Ag'(p_a)|} \qquad (44)$$

where A is a square matrix whose value depends on the chosen method, S is a positive scalar whose value is chosen so as to minimize $g(p_{n+1})$ and $g'(p_n)$ in the gradient sector of the functional g at the point p_n.

In the line of steepest descent method, it is important to transpose the position and gradient vectors into a standard set of units for height, position, and width. These are set at 0.1, 500, and 500 for peak height, position and width in the respective units. The units already balance in the Newton–Raphson method and do not need transposition, although the normalization is with respect to the above standard units.

The gradient vector is calculated as follows:

[37] L. M. Schwartz, *Anal. Chem.*, 1971, **43**, 1336.

$$\frac{\partial g}{\partial p_j} = \sum_i \left\{ \frac{\partial f(p_n), t_i}{\partial p_i} \left[f(p), t_i \right] - y_i \right\} \tag{45}$$

The matrix A is the identity matrix in the line of steepest descent method, whereas in the Newton–Raphson method it is calculated from:

$$(A^{-1})_j = \frac{\partial^2 g(p_n)}{\partial p_j \, \partial p_l}$$

$$= \sum_i \frac{\partial f(p_n, t_i)}{\partial p_i} \cdot \frac{\partial f(p_n, t_i)}{\partial p_l} + \frac{\partial^2 f(p_n, t_i)}{\partial p_j, \partial p_l} \cdot \left[f(p_n, t_i) - y_i \right] \tag{46}$$

The univariate search, *i.e.* the search to find the value of S so as to minimize $g(p_{n+1})$ proceeds by:

(i) Setting the value of S to zero.

(ii) The value of S is incremented by the *convergence factor* until a minimum $g(p_{n+1})$ is found.

(iii) The linear product of the (gradient vector at the new point) × (the direction of search) × (−1) is calculated and if it is negative the sign of the convergence factor is reversed.

(iv) The convergence factor is divided by 10.

(v) Repeat from step (ii) for a further sub-iteration.

The convergence factor at the start of each iteration and the number of subiterations per iteration may be set by the operator, or are otherwise set at 1 and 4, respectively. In the steepest descent method weights may be placed on each of the parameters, in which case the identity matrix is replaced by a diagonal matrix comprised of these parameters' weights. This allows certain parameters to be fixed and also allows certain parameters to vary more rapidly than others. These parameter weights do not apply in the Newton–Raphson method. The Gauss–Newton method is almost identical to the Newton–Raphson method described previously except that the second partial derivatives of the function $f(p_n,t_i)$ are ignored when calculating the A matrix.

Clearly, one method is more effective than others, a conclusion which has been dramatically shown by Pitha and Jones[38] in the reduction of fitting errors to a synthetic septuplet i.r. spectrum by a range of five methods. The effects of these methods when applied to fitting an u.v.–visible spectrum has not been explored, other than Levenberg's method.[39] In principle, fitting to Lorentzian (i.r.) and Gaussian (u.v.–visible) should be equally feasible, the only possibility being in the non-linearity of the parameters and the discrepancy between them and the linear Taylor series expansion approximation. In practice, the u.v.–visible and i.r. deconvolution problems are different by inspection, the number of bands in the u.v.–visible being less, but those bands being much broader and much more

[38] J. Pitha and R. N. Jones, *Can. J. Chem.*, 1966, **44**, 3031.
[39] K. Levenberg, *Quart. Appl. Maths.*, 1944, **2**, 164.

overlapped. Given the errors described at length previously, the convergence procedure will arrive at a 'global' minimum that satisfies equation (35).

Some control of the convergence procedure is necessary for operating on a series of overlapped absorption bands in the u.v.–visible region because powerful methods will reduce small bands to zero absorbance when they are adjacent to a large band and widen the large band to suit, creating a 'false' minimum. A sophisticated method of achieving convergence that may be used is to fix certain parameters for a few iteration cycles and then progressively to release parameters as an acceptable solution is approached. The method of constraining certain parameters may be either by direct specification or a 'window' technique on the partial spectrum allowing only certain bands to be converged. 'Band peeling' and 'sequential fitting' techniques fall into this category.

The philosophy of 'stripping', 'band peeling', and 'sequential fitting' supposes that the spectrum contains a dominant peak, which by definition assumes that the region immediately surrounding the band maximum is relatively free of contributions from other bands. This implies that the band shape is very close to a pure band shape; therefore this band can be removed by obtaining its parameters and then subtracting its contribution from the absorption. The accuracy of the analysis can be intuitively seen in the quality of the baseline which remains. This approach is very useful for dealing with the deconvolution of absorption profiles that have very intense, broad bands at, or just beyond, the spectroscopic limit of measurement.

5 Applications

Some applications of band shape analysis are now described in a varied selection of fields, emphasising the chemical aspects of these problems. Computer analyses are aids to our knowledge of chemical systems, not the primary objective, and should always be treated with healthy scepticism and discretion. The 'garbage in, garbage out' aphorism should always be remembered.

A. Magnetic Circular Dichroism.—Circular dichroism (c.d.) and magnetic circular dichroism (m.c.d.) spectra are presented as the difference between the absorption of left-handed and right-handed polarized radiation and the absorption profiles appear to follow Gaussian shapes as linear summations of both positive and negative bands, Figure 9, and also Figure 11a for the iodine visible band of the iodine–benzene charge transfer system in carbon tetrachloride.[40,41] The spectrum of the iodine–benzene complex was amongst the first of the type to be investigated and consists of the iodine spectrum, the charge transfer spectrum, and the benzene spectrum.[38]

There are many interesting facets of the spectra and we reluctantly confine ourselves to discussing the iodine spectrum. The gas phase iodine absorption band in the visible region has ν_{max} at 19 920 cm^{-1} and consists of three transi-

[40] A-G. El-Kourashy and R. Grinter, *J. Chem. Soc., Faraday Trans.* 2, 1976, **72**, 1860.
[41] R. S. Mulliken and W. B. Person, 'Molecular Complexes', Wiley Interscience, 1969, Section 105.

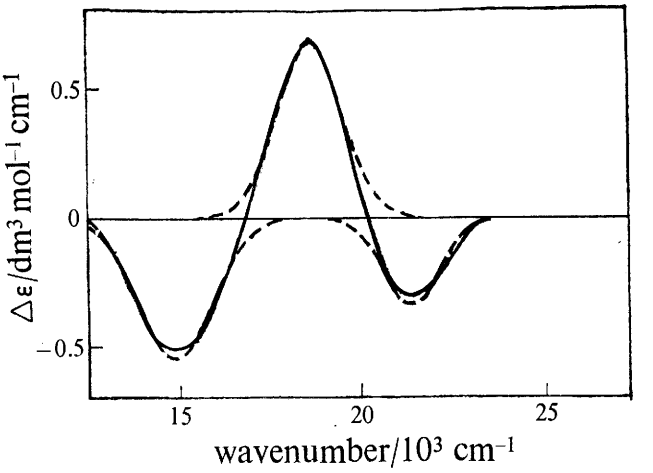

(a)

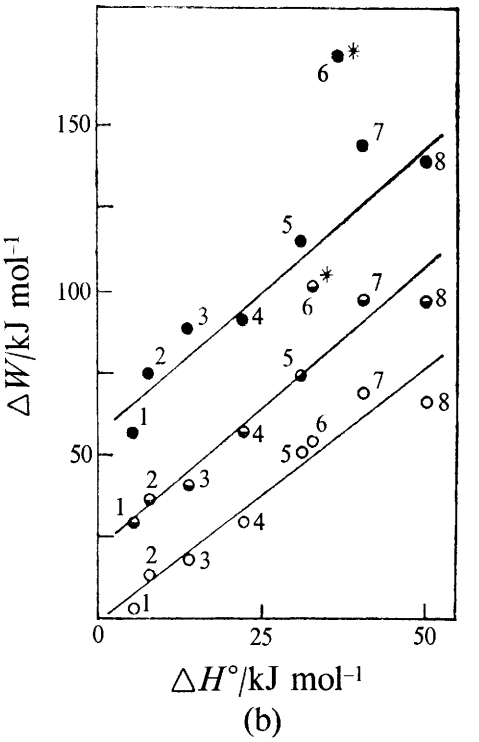

(b)

Figure 11 (a) *Gaussian analysis of the m.c.d. spectrum of the iodine visible band in the iodine/benzene complex in carbon tetrachloride, showing the experimental spectrum as the full line and the resolved bands together with the synthesized spectrum as broken lines.* (b) Plots of blue shift, ΔW, against enthalpy of complex formation: $-\Delta H^{\circ}$, *for the* $^{1}\pi_u$, $^{3}\pi + {}_{0}u$ and $^{3}\pi_{1}u$ bands, *from top to bottom, respectively, with the ordinates of the first two bands increased by* 25 *and* 50 kJ mol^{-1} *respectively, for clarity of presentation. The numbers given refer to those given in the text of ref.* 40

(Reproduced from *J. Chem. Soc., Faraday Trans.* 2, 1976, **72**, 1860)

tions,[41] $^3\pi_{1u}$, $^1\pi_{1u}$, $^3\pi+_{0u}$. These three bands are well separated and identified in the m.c.d. spectrum because their B terms have opposite signs, Figure 11a.[42] The charge transfer interaction of the iodine–benzene complex not only manifests itself in the charge transfer spectrum but also in positive shifts in ν_{max} and ϵ_{max} for the maximum of the iodine absorption bands. The blue shift can be correlated with the molar enthalpy of formation, $-\Delta H_f^\circ$, of the complex, although the correlation is rather scattered.[42]

The m.c.d. spectra of eight iodine/simple organic complexes were obtained, essentially similar to Figure 11a, and analysed using the ANGLIA program of Waddell[43] to obtain the three maxima and their shifts from their corresponding positions for iodine–cyclohexane alone. Plotted against $-\Delta H_f^\circ$ the maxima correlate well (except the two for pyridine, asterisked in Figure 11b) with increasing slope, *i.e.* in units of kilojoules,

$$^3\pi_{1u};\ \Delta W = 1.56\ \Delta H_f^\circ - 1.01 \quad (47)$$

$$^3\pi_{0u}^+;\ \Delta W = 1.66\ \Delta H_f^\circ - 3.99 \quad (48)$$

$$^1\pi_u;\ \Delta W = 1.88\ \Delta H_f^\circ - 6.24 \quad (49)$$

The computer analysis used Gaussian band shapes to fit the m.c.d. profiles. The analysis shifted the position of individual band maxima by up to 4000 cm^{-1} from the apparent maxima but the shift is most significant, in terms of the plot in Figure 11b, when the blue shifts are small. The correlations obtained using the resolved m.c.d. band maxima are considerably better than using the visible absorption maxima alone and hold for each of the components.

Mulliken[44] interpreted the blue shift as arising from the σ_u^* antibonding molecular orbital to which the electron is promoted within the complex being larger than the outermost occupied iodine molecular orbital in the ground state. The sudden increase in the size of the iodine molecule will increase the repulsion energy between the iodine and benzene components of the complex. The repulsion energy will be larger the more closely bound is the complex and must be added to the iodine transition energy; hence the blue shift increases with ΔH_f° for the complex.

Grinter and El-Kourashy[40] placed this interpretation on a more quantitative basis by considering the σ_u^* orbital to be similar to a Rydberg orbital. The electronic binding energy, E, of such an orbital will be inversely proportional to the radius of the excited state molecule. Therefore this radius will increase as the electronic binding energy becomes less negative, *i.e.* as the electron becomes less bound, and the blue shift will increase more rapidly with ΔH_f°. However, there must be limits as ΔH_f° will not decrease indefinitely as the distance between donor and acceptor decreases. Similarly the repulsion energy must tend to a limit as the donor–acceptor distance decreases. Overall, the correlation of the m.c.d. component bands maxima with ΔH_f° holds well, the small progressive differences

[42] M. Boith, M. D. Rowe, O. Schnepp, and P. J. Stephens, *Chem. Phys.*, 1975, **9**, 57.
[43] Dr. R. E. Waddell, personal communication.
[44] R. S. Mulliken, *Recl. Trav. Chim. Pays-Bas*, 1956, **75**, 845.

in the correlation for the separate components being consistent with Mulliken's original interpretation.

B. Evaluation of Tautomeric Equilibria in Biochemical Systems.—Band shape analysis and curve fitting is extremely onerous and can only be done for a large number of spectra if computer methods are used. Metzler *et al.*[11,45] have applied a highly developed computer method (LOGFIT) using the log-normal band shape to the electronic spectra of many compounds of biochemical interest.[46–49]

The log-normal band shape has since been shown to be better (more appropriate) than Gaussian band shapes and can be used to show up vibrational fine structure in absorption bands,[43] as in protein spectra.[44] The 3-hydroxypyridines[42] are related to vitamin B_6 and their spectra are of interest because of their various ionic states that can be obtained in a sequential manner. Figure 12 shows the spectra of the three ionic forms of pyridoxine as a particularly good example of how the spectra change from the cationic (H_2P) neutral (HP), and anionic (P) forms. A range of related compounds were studied, *i.e.* pyridine, pyrazine, phenol, and a series of substituted 3-hydroxypyridines, and the absorption profiles resolved in the manner of Figure 12 using the LOGFIT program.[11,47] Striking regularities appear when the results for each band are tabulated. Thus, for band I (the lowest frequency band of each set in Figure 12) the bandwidths and skewness values are remarkably uniform for given types of ion. The bandwidths for 15 3-hydroxypyridine cations averaged 3260 $\pm$ 60 cm^{-1}. Pyridine cation has a slightly narrower bandwidth of 3200 cm^{-1}, whereas methylation of the phenolic group narrows band I to 3090 cm^{-1}. Isopropylidine ring formation narrows the bandwidth further to 3010—3040 cm^{-1} whereas the only unusually wide cation band at 3490 cm^{-1} is found for isopyridoxamine phosphate. Averaged over all 20 cations the bandwidth is 3230 $\pm$ 120 cm^{-1}.

Dissociation of the phenolic hydrogen to the dipolar ion gives a 3—6% increase in bandwidth for band I to 3390 $\pm$ 90 cm^{-1} over 13 compounds and further dissociation gives a further increase in bandwidth of 3—4%, to 3630 $\pm$ 140 cm^{-1} over seven compounds. However, an interesting and contrary trend is shown by anions of pyridoxamine derivatives which narrow to 3220 cm^{-1} $\pm$ 20 cm^{-1}, relative to the dipolar ions. Some neutral forms were measured but in all cases the band was slightly broadened from that of the cation, consistent with the loss of a proton from the nitrogen.

Striking as the trends in bandwidth are, the skewness values for band I are even more uniform, for cations $\rho = 1.45 \pm 0.02$ (over 14 cations), for thirteen dipolar ions $\rho = 1.36 \pm 0.02$, whereas ρ for the seven anions is essentially

[45] D. B. Siano and D. E. Metzler, *J. Chem. Soc., Faraday Trans.* 2, 1972, **68**, 2042.
[46] D. E. Metzler, C. M. Harris, R. J. Johnston, D. B. Siano, and J. A. Thomson, *Biochemistry*, 1973, **12**, 5377.
[47] D. E. Metzler, C. M. Harris, I-Y. Young, D. N. Siano, and J. A. Thomson, *Biochem. Biophys. Res. Commun.*, 1972, **46**, 1588.
[48] D. E. Metzler, D. B. Siano, I-Y. Young, and C. M. Harris, *Fed. Proc., Fed. Amer. Soc. Exp. Biol.*, 1973, **32**, 661.
[49] D. E. Metzler and E. E. Snell, *J. Am. Chem. Soc.*, 1955, **77**, 2431

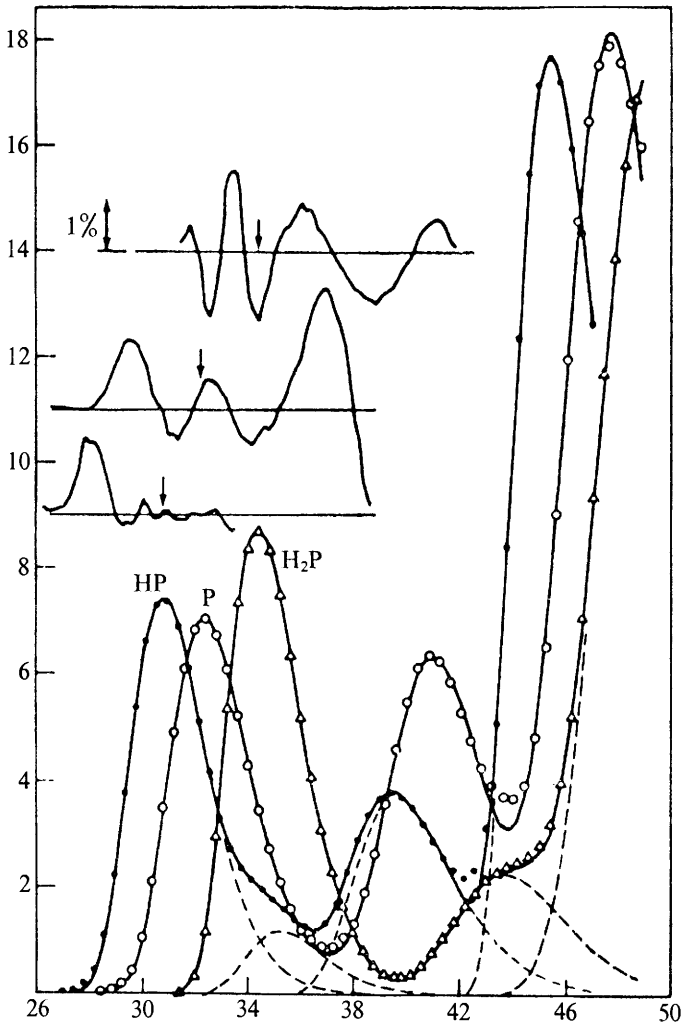

Figure 12 *The spectra of three ionic forms of pyridoxine represented as sums of log-normal curves, where* H_2P *is the cation,* HP *the neutral form (as the dipolar ion plus small amounts of the uncharged form), and* P *the anion form. The difference plots are given above the spectra for each summation, i.e. for each spectrum the difference between the observed spectrum and the sum of the log-normal component curves*
(Reproduced by permission from *Fed. Proc. Fed. Amer. Soc. Exp. Biol.*, 1973, **32**, 661)

unchanged at 1.37 ± 0.05. The band I skewness parameters of the pyridoxamine compounds are not significantly different except in the anion form where ρ = 1.43 ± 0.03. Neutral forms have substantially higher skewness values (1.52—

1.60) than for the cations. Similar trends are found for the parameters of bands II and III. An important observation was that areas of individual absorption bands are constant with changes in solvent composition or temperature.

A new method of evaluating tautomeric equilibria has been developed.[46] In order to resolve closely adjacent peaks of disparate intensities it is often necessary temporarily to fix the value of ρ, and sometimes the bandwidth in addition, for the less intense band so as to obtain an excellent fit to the absorption profile. Once the problem of resolving the profile has been overcome, the area for each band is computed for each solution. The tautomeric ratio, K_z, of the mole fraction of dipolar ion, f_z, to neutral, f_n, forms in water is given by:

$$K_z = f_z/f_n = \frac{a_z\, a_n{}^0}{a_n\, a_z{}^0} \tag{50}$$

where a_i and a_i^0 are the actual areas present and the molar area, respectively, and $f_z + f_n = 1$. The problem is that a_i^0 values are not normally directly measurable for tautomeric mixtures. However, as these values are constant with change in solvent composition but the tautomeric equilibrium will be varied, then a_i^0 values can be obtained by varying the solvent comparison. Thus if a_n is changed by a small increment Δa_n and similarly a_z changes by Δa_z, caused by a small shift in solvent composition, then:

$$\frac{\Delta a_n^0}{\Delta a_z} = \frac{a_n^0}{a_z^0} \tag{51}$$

and

$$K_z = (-\Delta a_n/\Delta a_z)(a_z/a_n) \tag{52}$$

following directly from the constancy of a_n^0 and a_z^0 and assuming only two tautomeric species. One of the a_i^0 values can be obtained with confidence in one of the pure solvents of the mixture and K_z calculated from a series of spectra in a mixed solvent system of varying composition. From the values of pK_a and K_z, microscopic dissociation constants of the —OH and =NH+ groups were evaluated, which are of considerable importance in biology. The trend of values obtained for a range of related compounds was much more consistent than previous values. The main reason for the improvement was that previous methods had not used band areas, but intensities, or had not allowed for the effects of other bands present by not resolving the profiles completely.[46]

C. Rigour, Internal Linearity, and Isosbestic Points.—Experimental conditions such as temperature, ionic strength, and/or pH are often incrementally adjusted to study a chemical equilibrium. The presence of an isosbestic point is generally regarded as evidence for the number of reacting species or independent reaction parameters. An important caveat is underlined by the rigorous demonstration that isosbestic points generated by environmental perturbation are formed under a much wider variety of conditions than had been previously

recognised.[50,51] Therefore the rules proposed[52–54] for interpreting systems which show isosbestic points are unreliable and can break down in certain cases. In most applications it is more useful to show that spectra are linearly related, see below, than to show that they have isosbestic points. As one instance, temperature effects give particular problems because the individual component spectra will vary in intensity, position, and width with temperature, therefore the reference, *i.e.* 'pure' spectra, will vary in addition to the temperature-dependent equilibria between the component species.

Griffiths and co-workers[7] were the first to apply computer deconvolution methods to sets of equilibria obtained for chemical systems perturbed by temperature change in conjunction with tests for internal linearity. They have concentrated on transition-metal ions in equilibrium with inorganic anions in dimethyl sulphoxide.

The test for internal linearity follows from considering a two-species equilibrium to be present in solution, with the total concentration of the two absorbing and interacting species remaining constant.[7] If the relative concentrations of the two species are altered by an externally applied constraint, then the spectra will normally contain at least one isosbestic point and are regarded as internally linear. It follows that any one spectrum in an internally linear set is a linear combination of any other two spectra from that set, expressed as:

$$\epsilon_3 = (1 - \beta)\,\epsilon_1 + \beta\epsilon_2 \qquad (52)$$

which should be valid at any wavelength within the internally linear range; ϵ_1 and ϵ_2 are termed the reference spectra and β is the constant of internal linearity relative to the spectra ϵ_1 and ϵ_2. Rearrangement of equation (52) gives β_λ as,

$$\beta_\lambda = (\epsilon_3 - \epsilon_1)/(\epsilon_2 - \epsilon_1) \qquad (53)$$

implying that the constant of internal linearity is calculated at each wavelength. An average value, $\bar{\beta}$, is then calculated and, if meaningful, the deviation from ideal linearity is calculated at each wavelength,

$$\Delta_\lambda = (1 - \bar{\beta})\epsilon_1 + \bar{\beta}\epsilon_2 - \epsilon_3 \qquad (54)$$

and the plot of Δ_λ against wavelength establishes both the magnitude and range for which the spectra can be regarded as internally linear. Limits have to be set when the influence of noise causes ϵ_1 and ϵ_2 to cross over fortuitously, making β oscillate between positive and negative large values. If β is changed in an incremental manner and the spectra redrawn then a situation will arise where one species is eliminated and the resultant is the terminal spectrum of the remaining species, which may then be compared with the resolved spectrum.

Central to this procedure is the computer analysis of the spectra using the fourth derivative method. Temperature has a profound effect on the co-ordina-

[50] J. Brynestad and G. P. Smith, *J. Phys. Chem.*, 1968, **72**, 296.
[51] E. P. Smith, C. R. Boston, and J. Brynestad, *J. Chem. Phys.*, 1966, **72**, 829.
[52] D. M. Cohen and E. Fischer, *J. Chem. Soc.*, 1962, 3044.
[53] J. R. Morrey, *J. Phys. Chem.*, 1962, **66**, 2169; 1963, **67**, 1569.
[54] C. A. Angell and D. M. Gruen, *J. Am. Chem. Soc.*, 1966, **88**, 5192.

tion of Ni^{II} in the Ni^{II}–chloride–dimethyl sulphoxide,[7] as can be seen from the spectra in Figures 13 (i) and 13 (ii). The fourth derivative spectra are super-

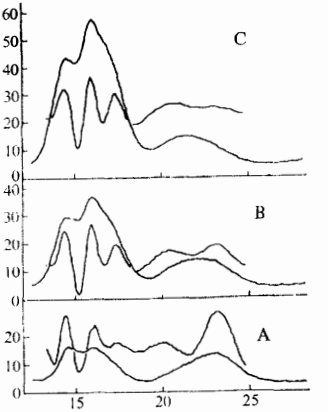

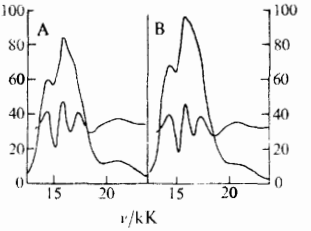

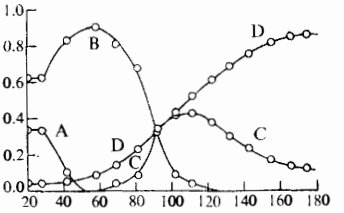

Figure 13 (i) *Absorption spectra and fourth-derivative functions of* Ni^{II} + 4.45M-Cl^- *solutions in DMSO recorded at* (a) 342.3 K, (b) 365.2 K, *and* (c) 384.5 K. *The derivatives are calculated by the method of differences from several integer sets.* (ii) *as in* (i) *but recorded at* (a) 416.3 *and* (b) 448.1 K. (iii) *The deduced variations in concentration of various* Ni^{II} *complexes in* Ni^{II} + 4.45 M-Cl^- *in DMSO from* 294.2 K *to* 448.2 K, *species denoted as* (a) $|Ni(DMSO)_6|^{2+}$, (b) $|NiCl(DMSO)_5|^+$, (c) $|NiCl(DMSO)_4|^0$, (d) $|NiCl(DMSO)|^-$

(Reproduced from *J. Chem Soc., Dalton Trans.*, 1975, 344)

imposed upon the actual spectra and clearly show the main peaks but also the shoulders at about 17 000 cm^{-1}. The bands at 14 560, 16 050, and 16 950 cm^{-1} increase with increase in temperature and are assigned to the $[NiCl_3(DMSO)]^-$ complex. The tetrachlorocomplex, $[NiCl_4]^{2-}$ has bands at 15 300 and 14 300 cm^{-1} and is clearly absent. The octahedral species reported in Ni^{II} + chloride in dimethyl sulphoxide has been shown to have single maxima in the visible region as:

$[Ni(DMSO)]^{2+}$	24 040 cm^{-1}
$[Ni(DMSO)_5Cl]^+$	23 000 cm^{-1}
$[Ni(DMSO)_4Cl_2]^0$	21 000 cm^{-1}

However, only one broad peak is observed above 20 000 cm^{-1}. The fourth derivative analysis gives the relative concentration of these bands. The additional bonus of the fourth derivative analysis is to give the relative concentrations of these species, plotted in Figure 13 (iii) showing the gradual transformation between the various Ni^{II}–chloride–DMSO species, as:

$$\underset{\text{octahedral}}{[Ni(DMSO)_6]^{2+}} \overset{K_1}{\rightleftharpoons} \underset{\text{octahedral}}{[NiCl(DMSO)_5]^+} \overset{K_2}{\rightleftharpoons} \underset{\text{octahedral}}{[Ni(DMSO)_4Cl_2]^0} \overset{K_3}{\rightleftharpoons} \underset{\text{tetrahedral}}{[NiCl_3(DMSO)]^-} \quad (55)$$

An interesting effect is that the 'shoulder' observed for the lower temperature spectra in the region of 17 000 cm^{-1} is consistently analysed by the fourth derivative method for all spectra to be at 17 384 ± 23 cm^{-1}. A further development of this approach used the method of internal linearity to determine ΔH_f° for the reaction:

$$\underset{\text{octahedral}}{[Ni(DMSO)_4Cl_2]^0} \rightleftharpoons \underset{\text{tetrahedral}}{[NiCl_3(DMSO)]^-} \quad (56)$$

D. The Solvated Electron.—The solvated electron is under continuing scrutiny as one of the major current problems in solution chemistry and spectroscopy.[55] An important feature of solvated electron spectra is the asymmetry of the band that is strongly skewed towards high energies. The asymmetry varies from one solvent to another. Lugo and Delahay[56] resolved the absorption profiles of the solvated electron in five solvents at ambient temperatures and one solid system at 77 K using a mixture of bands and band shapes. The bands were constrained to have the same widths in this work. The different band shapes arise from the assumption of several bound–bound (b–b) and one bound–continuum (b–c) transitions, supported by recent theoretical work.

Freeman and Jou[57] measured the spectrum of solvated electrons in water, alcohols, and tetrahydrofuran over a wide range of wavelengths so as to improve the quality of wavefitting in the wings of the bands. Figure 14a shows the resolution of the solvated electron spectrum in ethanolamine at 299 K as two Gaussian bands and a continuum tail to higher energies.

[55] 'Electrons in Fluids', issue, *Can. J. Chem.*, 1977, vol. 55.
[56] R. Lugo and R. Delahay, *J. Chem. Phys.*, 1972, **57**, 2122.
[57] G. E. Freeman and F. Y. Jou, *Can. J. Chem.*, 1977, **57**, 591.

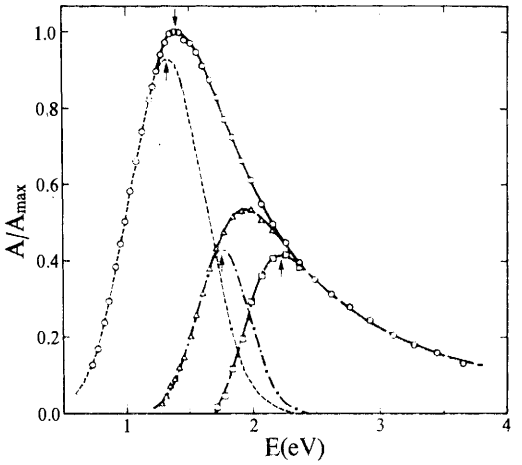

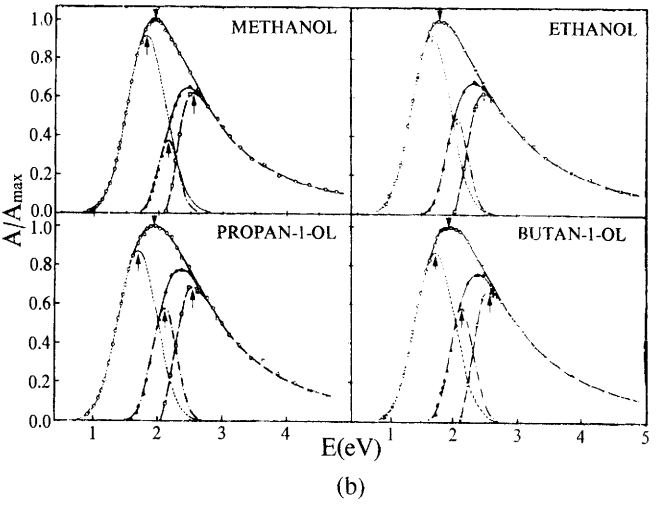

Figure 14 (a) *The band resolution of the optical absorption spectrum of solvated electrons in ethanolamine at* 299 K: 0,*experimental;* △, *first remainder:* □, *second remainder;* – – –, *first Gaussian;* –·–·–·, *second Gaussian;*— — —, *continuum tail;* ↓, *spectrum maximum;* ↑, *band maximum.* (b) *Band resolution in methanol, ethanol, propan-1-ol, and butan-1-ol at* 299 K, *symbols as above*

The band fitting starts from the low energy side of the spectrum by transforming the Gaussian equation of the *i*th band into a linear form as:

$$\ln A = \ln A_{\max,i} - (\ln 2/g^2)(E_i - E)^2 \text{ for } E < E_i,\ i = 1 \text{ or } 2 \qquad (57)$$

A is the absorbance at energy E (in eV), $A_{\max}$ is the maximum absorbances at position E_i, and g_i is half the width of the ith band at $0.5A_{\max,i}$. Final values of E_i, g_i, and $A_{\max,i}$ are obtained from the equation that provides the largest correlation factor. This first Gaussian is subtracted from the whole spectrum to obtain a remainder, which is then fitted with a second Gaussian. (A third Gaussian, if it exists, would have a very narrow width.) A high energy tail is left. The results of the procedure described above are shown in Figure 14a for the solvated electron in ethanolamine at 299 K.

Figure 14b shows similar resolutions of solvated electron spectra in methanol, ethanol, propan-1-ol and butan-1-ol at 299 K.

In alcohols and water the halfwidths for the first and second Gaussians are 0.71 ± 0.07 eV and 0.37 ± 0.08 eV, and the width at half height of the high energy tail is 1.0 ± 0.2 eV.

The first Gaussian band is assigned to a bound–bound transition, based on the fact that photobleaching of trapped electrons in organic glasses[58–60] ice,[61] and liquid methanol[62] have a very low quantum yield for photon energies on the low energy side of the absorption maximum. Photoconductivity[63–66] and stimulated luminescence[67] phenomena support this approach. It would be consistent for the excited state of the transition to be bound by the same potential well as the ground state, the low quantum yield being assigned to either thermal agitation or tunnelling from the excited state through to the continuum.

The second Gaussian is assigned to a transition to a higher electronic state. Its oscillator strength is lower, overall contributing less than 10% to the total for the whole band.

The continuum tail has a rapidly ascending and slowly descending absorption *versus* energy curve and is very similar to the photoionization spectrum of direct bound–continuum transitions. The band resembles the detrapping curves of photobleaching quantum yield, photoconductivity, and stimulated luminescence intensity.[58–67]

Overall, the band system is described by analogy to the hydrogen atom as the first Gaussian being a $1s \rightarrow 2p$ transition, the second to a $1s \rightarrow 3p$ transition, and the high energy tail to $1s \rightarrow$ continuum. For hydrogen atoms, the oscillator strengths were calculated as $f_{1s\rightarrow 2p} = 42\%$, $f_{1s\rightarrow 3p} = 8\%$, and the sum of other transitions as 50%.[68] By comparison, for all alcohol liquids (except for

[58] A. Bernas and D. Grand, *Chem. Commun.*, 1970, 1667.
[59] A. Habenbergenova, L. Josimovic, and J. Teply, *Trans. Faraday Soc.*, 1970, **66**, 656,669.
[60] H. B. Steen and J. Moon, *J. Phys. Chem.*, 1972, **76**, 3366.
[61] K. Kawabata, *J. Chem. Phys.*, 1971, **55**, 3672.
[62] A. Bromsberg and J. K. Thomas, *J. Chem. Phys.*, 1975, **63**, 2124.
[63] K. F. Baverstock and P. J. Dyne, *Can. J. Chem.*, 1970, **48**, 2182.
[64] T. Huang, I. Eisele, D. P. Lin, and L. Kevan, *J. Chem. Phys.*, 1972, **56**, 4702.
[65] T. Huang and L. Kevan, *J. Am. Chem. Soc.*, 1973, **95**, 2122.
[66] S. A. Rice and L. Kevan, *J. Phys. Chem.*, 1977, **80**, 847.
[67] A. Bernas, D. Grand, and T. B. Truong, *J. Chem. Soc., Chem. Commun.*, 1972, 759.
[68] H. A. Bethe and E. E. Saltpeter, 'Quantum Mechanics of one- and two-electron atoms', Academic Press, New York, N.Y., 1957.

t-butanol, which has other odd features) the distribution of oscillator strengths is 33%, 10%, and 55%. In water the distribution is 69, 8, and 23% respectively.

The results of this work, based upon a stepwise deconvolution and fitting procedure, show a set of discrete overlapping bands and a continuum which are in agreement with the recent theoretical work of Banerjee and Simons.[69]

E. Halide Solution Spectra.—The solution spectra of simple inorganic ions show intense absorption bands in the u.v. region, *e.g.* aqueous iodide has absorption maxima at 226 and 195 nm (298 K) with oscillator strengths of 0.25 and 0.28 respectively, Figure 15. Other simple anions show a similar series of transitions, characterized by Smith and Symons[70], as 'charge-transfer-to-solvent' (CTTS), developing previous work by Platzman and Franck.[71] The transition is simply written as:

$$X^-_{aq} \xrightarrow{h\nu} [X + e^-]_{aq} \tag{63}$$

where [ ] represents the solvent cavity of the original ion. The excited state therefore consists of the radical, X, and the solvated electron centred on the parent anion site. X may exist as one of several energy states, such as the $^2P_{\frac{1}{2}}$, $^2P_{\frac{3}{2}}$ states of the halides. Symons *et al.* showed that the bulk properties of the solvents used could not explain the dramatic effects of solvent, temperature, pressure, and electrolyte and therefore introduced the concept of a variable cavity radius parameter, r_d, which explains the environmental effects extremely well. The energy maximum, $h\nu_{max}$, is given by:

$$h\nu_{max} = IP(X^-) + \frac{h^2}{8mr_0^2} \tag{64}$$

A slightly divergent development from the Platzman and Franck model culminated in the extended model of Treinin for multivalent anions,[72] *e.g.*

$$X^z{}_{solv} \rightarrow X^{(z-1)-} + e^-{}_{aq} \tag{65}$$

Many studies have been carried out on the CTTS spectrum of iodide mainly because its spectrum is so accessible. In a concentration of 5×10^{-5} mol dm^{-3} it will have an absorption maximum of 0.7 in a 10 mm cell in water. At such a low concentration the spectrum of solvated iodide acts as a 'microprobe' of its environment. Iodide has been so used to study the environmental effects of temperature, pressure, added co-solvent, electrolyte, and non-electrolyte on solution structure. A wealth of data have been reported, that up to 1969 being reviewed by Blandamer and Fox.[73] Almost all of the solution/environmental studies refer to the first, lowest energy absorption band of iodide, at 226 nm in aqueous solution.

Attention has now turned to higher energy, further CTTS bands and their

[69] A. Banerjee and J. Simons, *J. Chem. Phys.*, 1978, **68**, 415.
[70] M. Smith and M. C. R. Symons, *Trans. Faraday Soc.*, 1957, **53**, 338, 346.
[71] R. L. Platzman and J. Franck, *Z. Phys.*, 1954, **138**, 411.
[72] A. Treinin, *J. Phys. Chem.*, 1963, **67**, 893.
[73] M J Blandamer and M. F. Fox, *Chem. Rev.*, 1970, **70**, 59.

inter-relationships. The problem of observing these bands in solution arises from their position in the far-u.v. region. Solid and vapour spectra are well reported for the far-u.v. region but techniques for measuring *solution* spectra in the 200—160 nm region needed to be developed such that they could be recorded on a routine basis.[74] A further problem was that the spectra consisted of extensively overlapped absorption bands.[75] The extent of overlap could be reduced by moving to considerably lower temperatures such that the bands were narrower

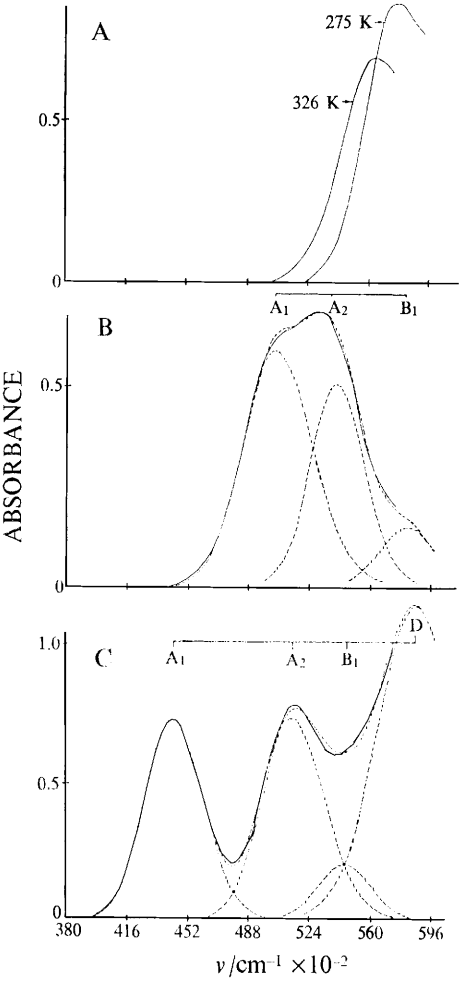

Figure 15 (i)

[74] M. F. Fox, *Appl. Spectrosc.*, 1973, **27**, 155.
[75] M. F. Fox and E. Hayon, *J. Chem. Soc., Faraday Trans.* 1, 1977, **73**, 1003; *Chem. Phys. Lett.*, 1972, **14**, 442.

and overlap thereby reduced. A series of techniques were developed to resolve the bands using analogue and digital methods. The log-normal band shape, with a skewness parameter close to 1.0 was shown to fit the data better than the normal, Gaussian, band shape, particularly so when used as a linear summation for complex absorption profiles.[4]

The most interesting, and controversial, observation has been the resolution of a low intensity band, B_1, (in red-shifting solvents a low intensity band pair) in addition to the well-defined, high intensity bands. The evidence for the existence of these bands rested upon a number of factors. First, unsatisfactorily synthesized resolutions were obtained in their absence.[4] Secondly, when using log-normal (skewed) bands and also excluding these bands, the two components of the major doublet pair would have pronounced skewness values of *opposite* slope, which is not reasonable.[4] Third, these bands were not only found for iodide in a range of solvents, where a pattern of solvent sensitivities and band intensities were demonstrated, but similar patterns found for bromide, chloride, and hydrosulphide band profiles,[75–78] Figure 15. Moreover, the existence of a series of bands for the halides and the solvated electron (as it eventually became)

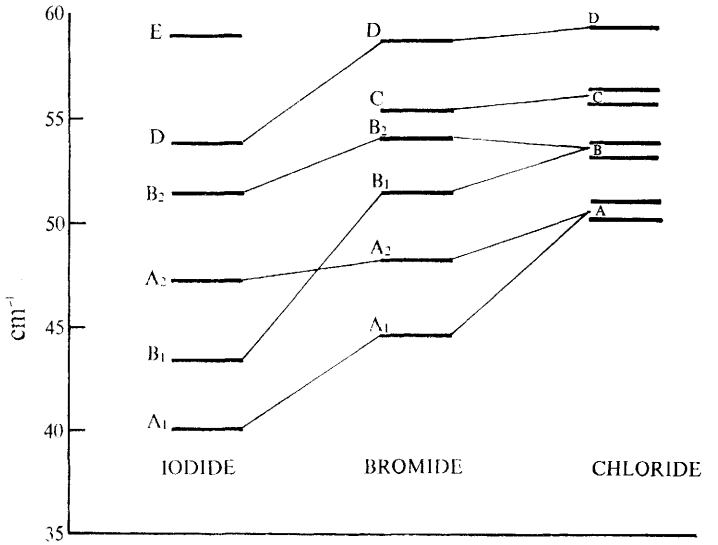

Figure 15 (ii)

Figure 15 (i) *The far-u.v. spectra of the halides in aqueous solution at* 5 × 10^{-3} mol dm^{-3}, (a) *chloride at* 275 *and* 326 K, (b) *bromide at* 318 K, *and* (c) *iodide at* 274 K; *and* (ii) *the relationship between energy levels for the halides in propionitrile at* 298 K
(Reproduced from *J. Chem. Soc., Faraday Trans.* 1, 1977, **73**, 872)

[76] M. F. Fox and E. Hayon, *J. Chem. Soc., Faraday Trans.* 1, 1977, **73**, 872.
[77] M. F. Fox, B. E. Barker, and E. Hayon, *J. Chem. Soc., Faraday Trans.* 1, 1978, **74**, 1776.
[78] M. F. Fox and E. Hayon, *J. Chem. Soc., Faraday Trans.* 1, 1979, **75**, 1380.

was predicted by Franck and Platzman as a Balmer-type series in the doctoral thesis of Platzman in 1942.[79] These additional bands appear to fit this prediction, though they do not converge exactly as predicted in terms of intensity and position. Further support is given by the observation of iodide spectra at very low temperatures in a mixed alkylnitrile solvent at 118 K, where the use of a band stripping technique for the first band gives unambiguous evidence for the existence of the B_1 band.[32]

In these studies we can see the deployment of a strategic analysis in depth, either through an initial analysis *via* LOGDIFF, PEAK, or an analogue/joystick method, followed by an optimization stage to give a good fit at the final, synthesized spectra to the original profile. In the latter analysis both normal (Gaussian) and log-normal band shapes have been used. 'Band peeling' has also been used where spectra are incomplete, particularly where high intensity bands appear to higher energies but beyond the limit of observation.

Finally the minimum number of bands rule has been applied, as has also the rule that resolutions must make chemical/physical sense. In the latter case, the two components of a doublet with sharply different skewness values for their band shapes has been rejected in favour of a solution where their skewness values are similar.

6 Future Trends

In this final section we look at, and speculate upon, techniques that will influence the future development of electronic absorption profile deconvolution.

We do not foresee dramatic changes in convergence/optimization procedures. It is evident that they vary in effectiveness according to the processes to which they are applied. It is further evident that the range of procedures described in Section 4 are best suited to optimizing the parameters of linear arrays of Gaussian/log-normal bands;[36] marginal improvements may be made but no dramatic changes are envisaged.

On the other hand, the techniques of factor analysis, as developed and applied by Shurvell and Bulmer[80] for the i.r. spectra of multicomponent systems, has not as yet been *successfully* applied to electronic absorption spectra. This technique can answer, given good data conditions, the central problem of how many bands contribute to an absorption profile. The technique is independent of band shape assumptions and applies to a set of constitutive properties for each of a series of NS solutions. The spectra are represented by a set of co-ordinates measured at NW (small) wavenumber intervals over an i.r. absorption band containing NC components and normalized to unit path length. The Beer–Lambert law normalizes absorbance values at given wavenumbers to molar absorption coefficients and concentrations of all components at that wavelength.

Matrix notation gives this as $A = EC$ where A is the (NW $\times$ NS) normalized

[79] R. L. Platzman, Ph.D. Thesis, University of Chicago, 1942.

[80] J. T. Bulmer and H. F. Shurvell, *J. Phys. Chem.*, 1973, **77**, 256; 'Molecular Spectroscopy of Dense Phases—Proc. 12th European Congress on Molecular Spectroscopy', Strasbourg, France. July 1-4, 1975, Elsevier, Netherlands.

absorbance matrix, E is the (MW × NC) molar absorption coefficient matrix, and C is the (NC × NS) concentration matrix. Shurvell and Bulmer used between 100—200 points for NW and 8—10 solutions for NS. Under these conditions it can be shown that the rank of the absorbance matrix is equal to NC provided that the spectrum of one of the components is *not* a linear combination of the spectra of the other components and that the concentration of one or more species cannot be expressed as a linear combination of the other component.

NC is the rank of the absorbance matrix and is found by calculating the eigenvalues of the matrix $A^{T}A$, where A^{T} is the transposition of A. This matrix has dimensions of (NS × NS) and the number of non-zero eigenvalues is equal to the rank of A. Owing to errors introduced by the reality of experiment and computing processes, all eigenvalues are generally non-zero and statistical tests have been applied to decide which are in fact non-zero. The results achieved from i.r. studies of systems in equilibrium have been impressive.

We have described the factor analysis technique at length because we feel that its potential application to the electronic absorption spectra of systems could be extremely valuable. The difficulty is that transfer of this technique to electronic spectra from the i.r. region is not straightforward because the conditions are different. The parameter varied most readily in electronic spectroscopy is the system temperature, which in turn readily affects the spectra of the pure components, as well as the equilibrium between those components. This is quite different from the i.r. studies where only concentrations have been changed. If the variation of the pure spectra can be overcome then factor analysis should become a powerful technique for resolving sterile controversies concerning the number of bands contributing to absorption profiles.

The deconvolution problem exists in other fields. It is interesting to note here techniques which could be, but have not been as yet, applied to resolving electronic absorption bands. Fourier-analysis of spectral line profiles has been reported by Bennett,[81] Smith and Gray,[82] and Karp,[83] amongst others. This promises to be a very powerful technique through the use of the Cooley–Tookey fast Fourier algorithm and associated hand-wired processors which can process a set of several thousand data points in less than one millisecond. Convergence method can then be applied.

Bayes' theorem in the field of conditional probability has been applied as the basis of a deconvolution algorithm by Kennett *et al.*[84] The applications described were mainly nuclear and X-ray spectroscopy work using a large array of channel detectors. Dose and Scheidt[85] have devised a stable and automatic method for resolving appearance potential spectra in the soft X-ray region. Hill[86] has

[81] W. R. Bennett, jun., *Appl. Optics*, 1978, **17**, 3344.
[82] M. A. Smith and D. F. Gray, *Publications of the Astronomical Society of the Pacific*, 1976, **88**, 809.
[83] A. H. Karp, *J. Quant. Spectrosc. Radiat. Transfer*, 1978, **20**, 379.
[84] T. J. Kennett, W. V. Prestwich, and A. Robertson, *Nuclear Instruments and Methods*, 1970, 285, 293, 153.
[85] V. Dose and H. Scheidt, *Appl. Phys.*, 1979, **19**, 10.
[86] R. M. Hill, *J. Quant. Spectrosc. Radiat. Transfer*, 1979, **21**, 19.

advocated the use of the 'curve of growth' to absorption line profiles. We draw attention to these activities in other fields to underline the point that the subject of this review is not unique and could benefit from parallel developments.

The current and well-established trend in u.v.–visible spectrophotometer design and development is to incorporate microprocessors so as to control the major functions of the machine. The subject of our review links directly with that trend by being the next natural development, either to provide feedback for control of the data gathering process, or as a data filter for onward transmission of the reduced band parameters to a multiaccess computer. Reduction of spectroscopic data to band parameters using the technique that we have described in this review is particularly important in automatic chemical analytical techniques.

A major thrust in the computing aspect will be the further development of interactive methods for resolving spectra, particularly if data are obtained on line. Gans has shown an integrated technique for fitting data using a light pen at an interactive graphics terminal.[30] On this terminal band parameters that have been estimated for a linear array of absorption bands may be varied using a light-pen—this corresponds to our definition of a first strategic level. Once a satisfactory fit has been achieved, a Gauss–Newton–Marquardt algorithm is used to converge the synthesized profile to the experimental curve by changing the band parameters. A difference curve is also plotted, enabling the areas of difference to be identified. In this way, very rapid deconvolutions may be achieved and the direction of subsequent experimental work decided upon much earlier—which is the point of the exercise!

A printout of the Leicester Polytechnic Deconvolution program,[26] which includes many of the techniques mentioned in this review, is available from the authors on request.